Study of a Non-Platinum-Based Antitumor Agent for Targeted Chemotherapy of Pancreatic Cancer

by

Xiaomeng Zhang

A thesis
presented to the University of Waterloo
in fulfillment of the
thesis requirement for the degree of
Master of Science
in
Physics

Waterloo, Ontario, Canada, 2021

AUTHOR'S DECLARATION

I hereby declare that I am the sole author of this thesis. This is a true copy of the thesis, including any required final revisions, as accepted by my examiners.

I understand that my thesis may be made electronically available to the public.

Abstract

Cancer has been a significant impediment to human life extension. Pancreatic cancer, the third largest cause of cancer mortality, presently lacks a viable therapy and is only detectable at a late stage. The advancement of femtobiology and femtochemistry facilitated the discovery of the exact molecular mechanism of action of the therapeutic anticancer medication. Our group discovered the mechanism of action of cisplatin, being the dissociative electron transfer (DET) reaction with a weakly bound (presolvated) electron. The research in femtobiology and femtochemistry led to the birth of a new frontier called femtomedicine (FMD). With the innovative FMD approach, our group discovered a novel family of non-platinum-based molecules (named FMD compounds) as anticancer targeting agents to replace the effective but highly toxic cisplatin. Overcoming the severe toxicity associated with the heavy metal Pt, these FMD compounds were shown to be effective anticancer agents in natural targeted chemotherapy and radiation therapy for various cancers. At the same time, they induced essentially no harmful side effects.

This thesis reports an in vitro evaluation of the therapeutic effect of one of the leading FMD compounds on pancreatic cancer. It presents the results of the anti-tumor efficacy and toxicity in pancreatic cancer cells and normal human cells, respectively, using four well-established cell-based test techniques. These assays include measurements of in vitro cell viability, cell death (reproductive ability), DNA DSB damage, membrane permeability, and apoptosis. The results show that as a potent antitumor agent, the FMD compound effectively reduced the cell viability by over 50 % at the FMD concentration of 300 μM and the reproductive capacity by over 60 % at 50 μM of pancreatic cancer cells. It was also observed by the fluorescent dye that the FMD compound induced visualizable severe DNA double-strand

breaks and apoptosis to pancreatic cancer cells. Compared with a clinical chemotherapy agent for pancreatic cancer patients, the tested FMD compound exhibited no significant drug resistance in *in vitro* experiments. Moreover, the treatment of the FMD compound induced negligible toxic effects on normal human cells, which remained 80 % of the cell viability at the FMD concentration of 300 μM and 80% of the reproductive capacity at 50 μM. These results confirm the low toxicity of the FMD compound, which will induce minimum side effects if applied in the clinic.

Overall, this study shows good promise of the FMD compound to become a targeted chemotherapeutic agent for pancreatic cancer.

ACKNOWLEDGEMENTS

I want to thank the following people. Without them, I would not have completed this research and made it through my master's project. I especially appreciate my supervisor Dr. Qing-Bin Lu, whose insight and knowledge into the subject matter continuously supported me through this research.

The depth of my appreciation goes to the members of my dissertation committee, Dr. Kesen Ma and Dr. Russell Thompson. They supported me during my master's studies and gave me valuable advice and help.

Special thanks also go to everyone in the great group. I want to express my gratitude to Chunrong Wang, Philip Chen, and Ning Ou for teaching me various skills and their helpful advice about the detailed designs of my experiments when I first joined this group. I would also like to thank all group members for their constructive discussions and generous contributions.

Above all, I could never appreciate enough my parents who believed in me and supported all my decisions, making me an independent and valuable person. Your love is keeping me alive in health and happiness.

Last but not least, I am thankful to the University of Waterloo, and the Department of Physics and Astronomy, which provided the opportunity for me to have this exciting experience for graduate study.

Table of Contents

List of Figures

List of Tables

Chapter 1 Introduction

1.1 The Significant of Cancer study

Cancer is one of the major diseases to influence the life expectancy of humans in the global burden. About 1 in every six deaths worldwide is caused by cancer, which is more than the total of tuberculosis, HIV/AIDS, and malaria combined (Hallquist, 2020). The American Cancer Society in 2020 stated in its annual report that cancer is the leading cause of premature death in the US working-age population (ages 20-65 years) (Hallquist, 2020). The report also estimates that by 2040, 27.5 million people in the world will be diagnosed with cancer, and 16.2 million people will die of cancer, solely depending on the population growth and aging population (Hallquist, 2020). As a low-survival rate disease, cancer is the second top leading cause of death (Figure 1-1, in 2017) globally. There were an estimated 225 800 new cancer cases in Canada and 83 300 cancer deaths in 2020 (Brenner, 2020). From the US Cancer statistics 2020, the estimated new cancer cases and deaths are respectively 1,806,590 and 606,520 in the United States in 2020 (Siegel, 2020).

Furthermore, the cancer cases are distributed in the age range of adolescents and young adults. In 2020, approximately 89500 adolescents and young adults of the United States were diagnosed with cancer (5,800 adolescents age 15-19 years; 83,700 young adults age 20-39 years), while there were 9270 cancer deaths in adolescent and young adults (Hallquist, 2020). These survived patients will have severer continued health effects, including sexual dysfunction, infertility, heart problems, and a high risk of future cancers. Therefore, even with the improved treatments and early diagnosis strategies, cancer study significantly impacts human life quality and longevity.

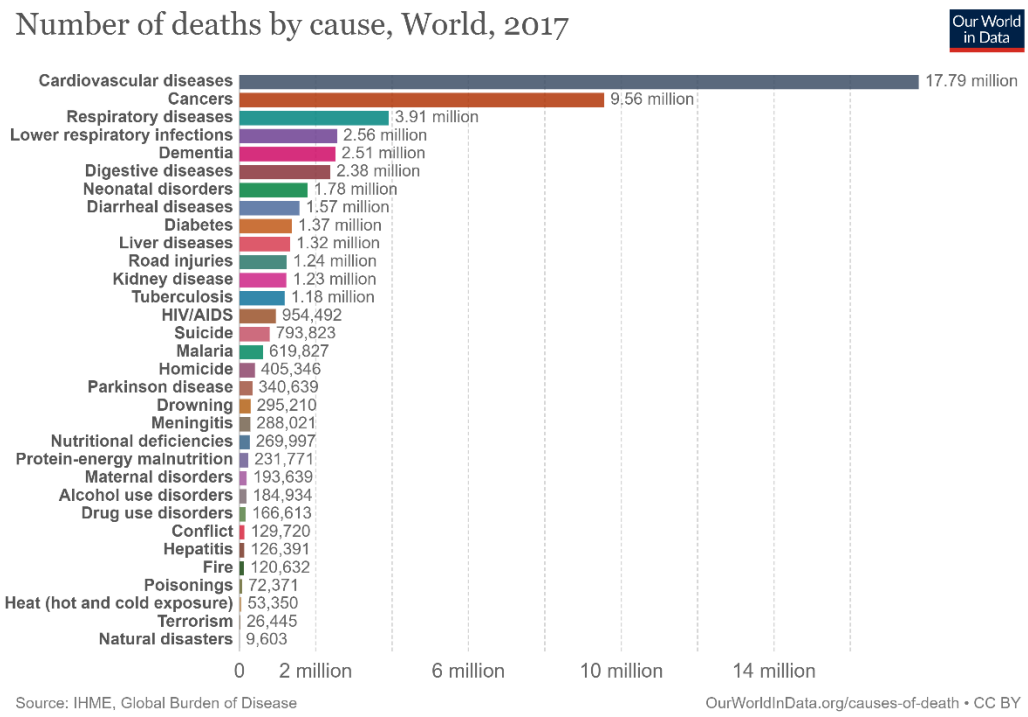

Figure 1- 1 Number of deaths by cause of the global burden in 2017. (Source IHME, Global Burden of Disease, https://ourworldindata.org/causes-of-death/)

1.2 Pathophysiology of Cancer

In general, cancer is caused by multiple changes in cells' specific genes related to fixing damaged DNA and controlling cell growth and division (Bray et al., 2018). The related genes include oncogenes and tumor suppressor genes (such as p53). Oncogene contributes to cell growth and reproduction, where the tumor suppressor gene inhibits them. The cancerization of cells would occur if there were multiple mutations of the affected genes, such as abnormal over-expression of oncogenes or disfunction of tumor suppressor genes. After the transformation, further mutations will accumulate during reproduction, further disorder apoptosis, accelerate cell division, or produce error signals to normal cells. Characteristic abilities of cancer cells tend to break through the limitation of tissue growth, become immortalized, and be increasingly

invasive. After excessive division, cancer cells will form the primary tumor. In the initiation stage of the tumor, cancer cells obtain advanced and steady features, including inactive to anti-growth signals, self-producing growth signals, angiogenesis, metastasis, rebuilt energy metabolism, and evasion immune destruction (Hanahan, 2011).

When the size of the tumor (diameter) reaches ~100 μm, there will be neovascularization in between tumor tissue to supply sufficient nutrients (de Wit, van Dalum & Terstappen, 2014). The tumor cells will have the opportunities to enter the circulatory and lymphatic systems, while the immune system will destroy most of them. However, the survived cancer cells will extravasate and invade the endothelial cell layer at different sites in the patient's body (Coghlin, 2010). These sites will start cancer cells proliferation and tumor angiogenesis progress, where the metastasis tumors will form. It is commonly known as late stages for cancer patients. At the late stage, multiple mutations appear at metastases (Figure 1-2), and the diversity of tumor cells increases, which brings more difficulties to cancer treatment.

A

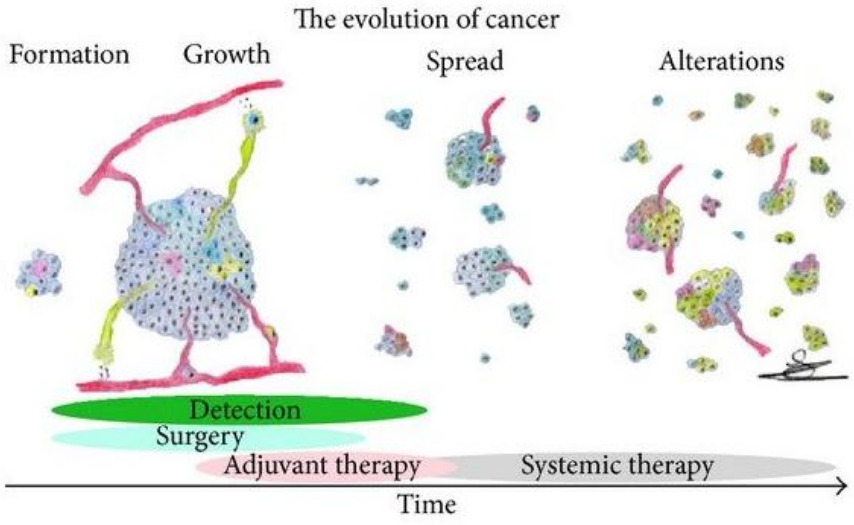

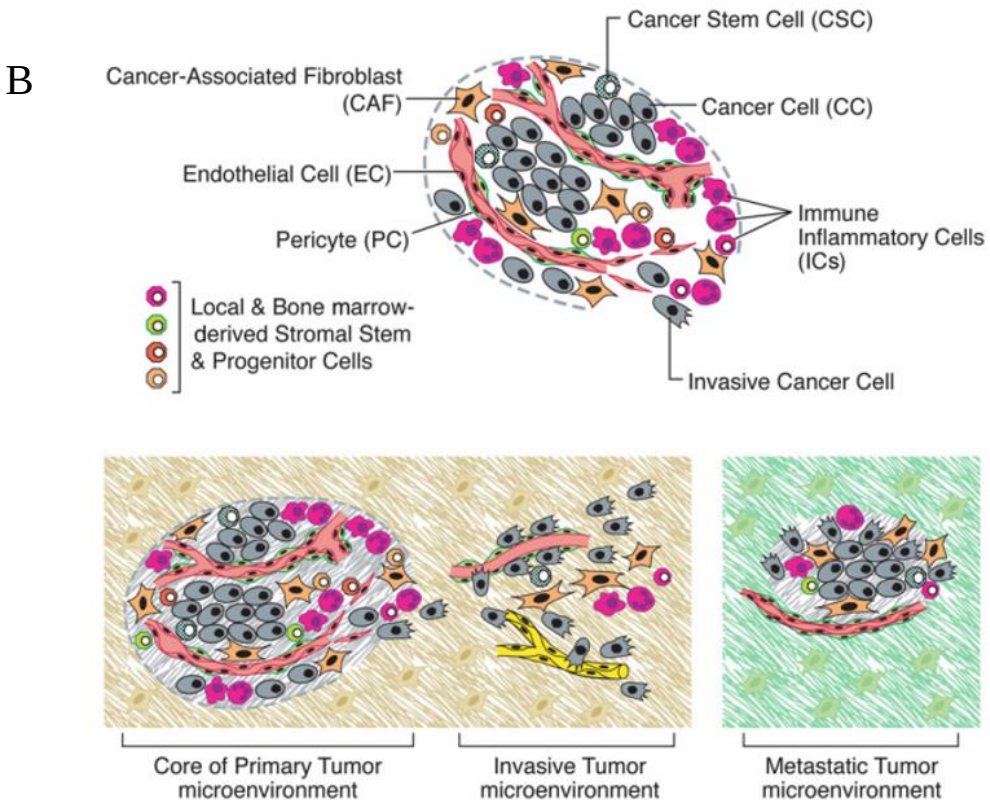

Figure 1- 2 The evolution of cancer. (A) After the initial formation of cancer cells, the tumor's expansion attracts blood vessels, which provide oxygen and nutrition. Cancer cells then travel through these veins, creating metastases in other parts of the body. (de Wit, van Dalum & Terstappen, 2014). (B) (Upper) An assemblage of distinct cell types constitutes most solid tumors. (Lower) The distinctive microenvironments of tumors. (Hanahan, 2011)

1.3 Cancer Diagnosis and Therapy

There have been various implemented diagnostic tools and treatments to detect or cure cancer or prolong patient life. For most types of cancer, the survival rate is much higher if the cancer is diagnosed at an earlier stage than at a late stage. For example, the one-year survival rate of colorectal cancer is 97.7% at stage 1, which drops to 43.9% if at stage 4 (Hawkes, 2019). So is ovarian cancer, for which 92% of patients survive for more than five years if diagnosed at stage

1, while diagnosed at stage 4, only 30% of patients survive over five years (Chien,2017). The one-year survival rate of liver cancer has a sharp decrease from 69.1% to 39.3% when the stage-2 patients develop into stage-3 cases (Hawkes, 2019).

Over the last 50 years, the armamentarium has been significantly developed for cancer diagnostic techniques in the clinic. Currently, the computed tomography (CT), magnetic resonance imaging (MRI), and ultrasonography could image the human body exquisitely in detail. These techniques assist in diagnosing cancer even before any clinical signs or symptoms (Histed, 2012). The development and prevalence of cancer screening detection have contributed to reducing the mortality of cancers including breast, uterine cervical, colorectal, prostate, and lung cancer (Sauer, 2019). However, certain types of cancer, such as pancreatic and ovarian cancer, hardly have any symptoms in the early stages and usually would not be diagnosed until advanced stages (distant metastasis). These cancer types have incredibly high mortality within five years after being diagnosed.

The development of cancer biomarkers gives a high potential for easier and more accurate diagnostic tools. For instance, evidence shows that the serologic autoantibody (to tumor-associated antigens, TAAs) level increases even precede the manifestation of cancer disease symptoms by several months to years, so that the autoantibodies are studied as diagnostic cancer biomarkers for early detection (AENKER, 2013). If the prostate-specific antigen (PSA) serum level of patients is higher than above four ng/mL, the patients have the potential to be diagnosed with prostate cancer (Stephan, 2007). Some biomarkers have been accepted for breast cancer diagnosis in the clinic, including carcinoma antigen, carcinoma antigen, and carcinoembryonic antigen (Brooks, n.d.). Autoantibodies MAPK9 (mitogen-activated protein kinase 9), CTDSP1 (carboxy-terminal domain, RNA polymerase II, polypeptide A, small

phosphatase 1), and NR2E3 (nuclear receptor subfamily 2, group E, member 3) have been recognized as potentially promising biomarkers of pancreatic cancer (Bracci, 2012). In practice, panels of multiple diagnostic autoantibody biomarkers are applied to improve sensitivity and specificity (AENKER, 2013).

After diagnosis, a combination of different cancer therapies will usually be applied according to the condition of the patients. These therapies take a critical role in extending the life of patients, which contains surgery, chemotherapy, radiation therapy, immunotherapy, targeted therapy, and hormone therapy. More likely, surgery is a palliative treatment, and it needs to be applied simultaneously with chemotherapy or radiation therapy. Targeted therapy is advanced chemotherapy without severe side effects. The medicines of this therapy have sensitive cytotoxicity to cancer cells and low effect on normal cells. It can target specific characteristics of cancer cells, such as tumor suppressor gene p53. Recently, immunotherapy has been quickly developed because of the study of cancer cell survival mechanisms. This strategy reactivates the detection/destruction targeting cancer cells by the immune system or counteracts the signal of cancer cells to avoid immune system detection. Therefore, there have been significant improvements in cancer therapies, and they are still under development.

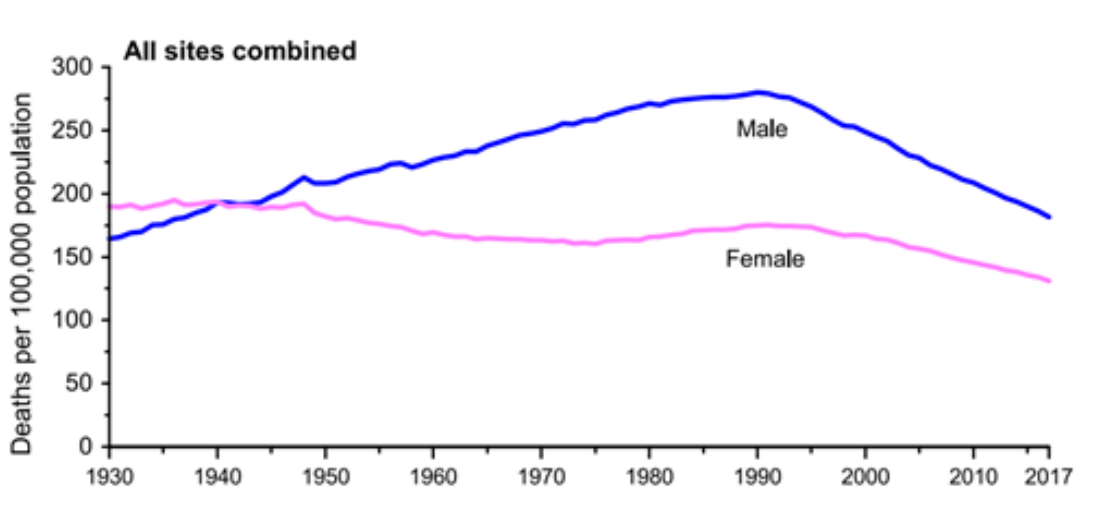

Figure 1- 3. Trends of all sites combined in Cancer Mortality Ratio by Sex, in the United States, 1930 to 2017. (Siegel, 2020)

The remarkable progress of early diagnosis and different cancer therapies have notably reduced the mortality of cancer patients. With improvements in early detection and different treatments, according to Fig.1-3, the mortality of cancer (all sites combined) has been sustainably declining since its peak of 215.1 deaths (per 100,000 population) in 1991 (Siegel, 2020). As of 2017, the overall reduction of 29 percent (152.4 per 100,000 population) is estimated 2.9 million fewer cancer deaths (around 1,983,000 males and 919,200 women) (Siegel, 2020). However, cancer is still a significant health problem worldwide.

1.4 Pancreatic cancer

As one of the most aggressive human cancer types, pancreatic cancer has been reported as the third leading cause (over breast cancer) of cancer-related deaths in Canada (Brenner, 2020) and the United States (Cancer Facts and Figures, 2017). It is reported that pancreatic cancer will be the second leading cause of death within a decade in Canada and the US, surpassed only by lung cancer (Zhang, 2018). In 2020, there will be an estimated 57,600 new cases of pancreatic cancer

in the US and 47,050 estimated deaths caused by this disease (Hallquist,2020), and around 6,000 new cases and 5300 deaths in Canada (Brenner, 2020). Even with the research efforts for this disease in recent decades, no significant improvements have been achieved. Pancreatic cancer remains the lowest survival rate among all cancer types. With current treatment, the median survival time is still less than 12 months, and the 5-year survival rate is still below 10% though it recently increased from 5% to 9% from 2017 to 2020 (Siegel, 2020).

In the localized stage, pancreatic cancer has no recognizable symptoms and signs. Consequently, most patients are not diagnosed until a late stage, after the cancer cells have metastasized to other organs (Figure 1-2A, 1-4) (Wolfgang, 2013). In the latter case, the surgical cure is no longer applicable. Clinically, since the late diagnosis, only 15% to 20% of pancreatic cancer patients are candidates for surgical resection. At the same time, the majority of them usually suffer from chemotherapy resistance, local recurrence, and metachronous metastasis (Felsenstein, Hruban & Wood, 2018). The five-year survival rate after pancreaticoduodenectomy, or Whipples procedure, is approximately 10–25% for patients, and up to around 71% of patients will have disease recurrence (Mizrahi et al., 2020). However, surgical resection of pancreatic tumors is the only treatment with curative potential for patients.

1.5 Histological Characteristics and Mutation Progress

The pancreas plays an indispensable role in regulating the body's metabolism. The pancreas is usually divided into three parts (head, body, and tail) (Figure 1-4), surrounded by the intestines, stomach, and spine. This vital gland secretes digestive enzymes for the small intestine through the pancreatic duct from the exocrine pancreas cells. It also produces various hormones into blood vessels, including insulin, glucagon, and somatostatin (by endocrine pancreas cells). About 95% of pancreatic cancers begin from mutated exocrine cells and end with ductal adenocarcinoma (Mizrahi et al., 2020). Only a few patients were diagnosed with neuroendocrine tumors.

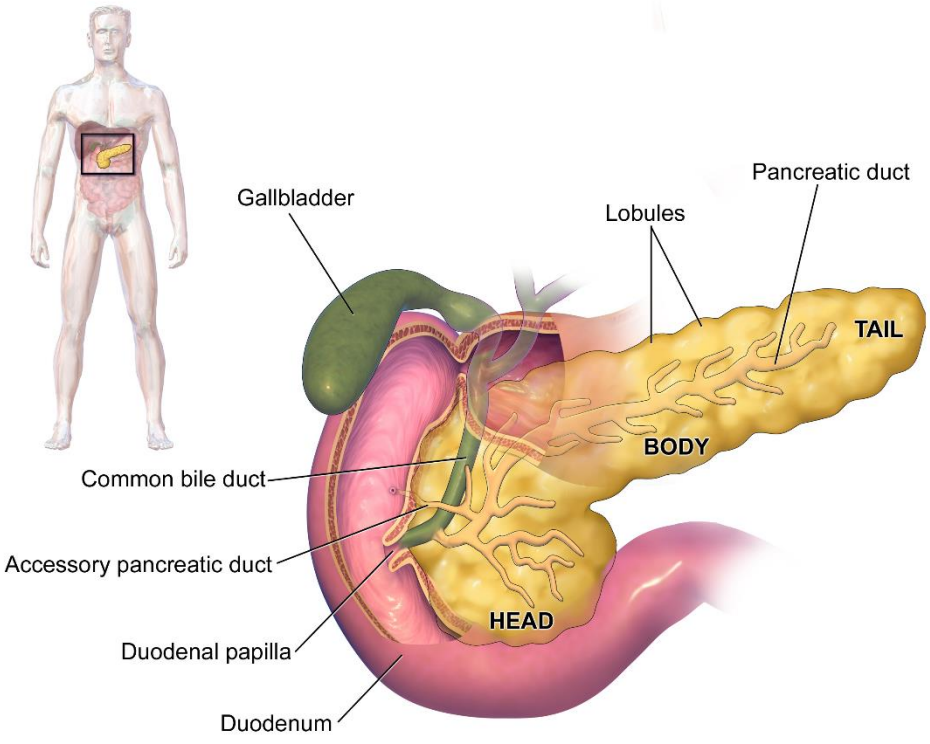

Figure 1- 4. The pancreas' anatomy. The pancreas is categorized into three sections: head, body, and tail. (Source: Medical gallery of Blausen Medical, 2014)

As mentioned before, the malignant behavior of cancer cells is caused by accumulated mutations in oncogenes and tumor suppressor genes of somatic cells (Stratton, 2009). Pancreatic ductal adenocarcinoma develops from non-invasive precancerous lesions. There are three most common precursor lesions with different histological features: PanIN, IPMN, and MCN, which are pancreatic intraepithelial neoplasia (<5mm), intraductal papillary mucinous neoplasm (>1cm), and mucinous cystic neoplasms, respectively (Felsenstein, 2018). Each of the distinct precursor lesions has its pathways to form pancreatic ductal adenocarcinoma. Figure 1-5 shows two different genetic alterations pathways PanIN and IPMN.

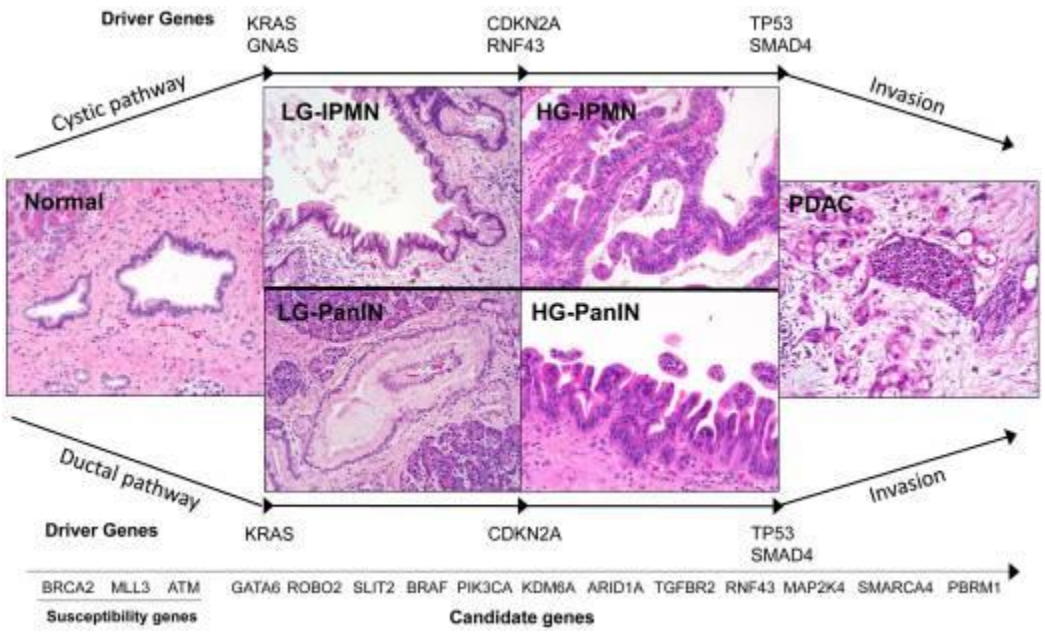

Figure 1- 5. The two different genetic alterations pathway of pancreatic ductal adenocarcinoma from two types of precursor lesions: pancreatic intraepithelial neoplasia (PanIN) and intraductal papillary mucinous neoplasm (IPMN). LG-PanIN and LG-IPMN are common low-risk precursors; HG-PanIN and HG-IPMN are more advanced precursors, with a high risk of transfer to invasive cancer. (Felsenstein, 2018).

In tumor progress arising from the PanIN precursor lesion, point mutations in the KRAS oncogene are found in over 90% of pancreatic ductal adenocarcinoma as an early event (Figure

1-5) (Singhi, 2019). The mutations in KRAS regularly occur at specific hotspot positions (codons 12, 13, 61), resulting in the activation of intracellular effector pathways, followed by cell cycle progression and increased cell survival and motility (Kanda, 2012; Caldwell, 2012). The mutated gene is associated with the inactivation of two cyclin-dependent kinase inhibitors (CDKN2A and CDKN1A) (Mizrahi et al., 2020), contributing to the transition to high-grade dysplasia. In the later stage, aberrations will occur to tumor suppressor gene TP53 (observed in 50–70%) and SMAD4 (60–90% of these malignancies) (Guo, 2016). The latter mutations would predominantly drive invasiveness (Hosoda, 2017).

The IPMNs lesion pathway partially overlaps with the PanIN pathway and has a different mutation at each step (Figure 1-5). The genetic alterations driving the formation of IPMNs are associated with activating mutations in the oncogene GNAS and inactivating mutations in the tumor suppressor gene RNF43 (Figure 1-5) (Amato, 2014). Mutations in TP53 and SMAD4 also play an essential role in malignant progression for IPMN-associated invasive carcinoma (Fig.1-5) (Kanda, 2013). MCN is the least prevalent preinvasive pancreatic lesion among all three precursor lesions. The mechanism of MCNs formation is similar to the pathway of IPMNs, except that GNAS alterations would not occur to MCNs. There is a common principle among all three precursor lesions. The tumorigenesis is initiated by the early oncogene mutations and the later loss of tumor suppressor genes (Felsenstein, 2018). The most frequently altered genes in pancreatic ductal adenocarcinoma are the oncogene KRAS and the three tumor suppressor genes TP53, CDKN2A, SMAD4. A better understanding of the genomic alterations in pancreatic neoplasms gives the potential to drastically improve early detection in clinic implications (Feigin, 2017).

1.6 Clinically treatment plan for pancreatic cancer

In order to plan the treatment after diagnosis, patients with pancreatic cancer can be staged according to the Cancer Staging Manual from American Joint Committee. More practically, the following groups are used to plan treatment in the clinic based on tumor resectability (Table 1-1): resectable pancreatic cancer, borderline resectable pancreatic cancer, locally advanced pancreatic cancer, metastatic pancreatic cancer, and recurrent pancreatic cancer (according to National Cancer Institute).

	Recommended management	Evidence	Comments
Resectable	Surgical resection → 6 months of postoperative chemotherapy or preoperative chemotherapy with or without chemoradiotherapy → surgical resection → postoperative chemotherapy	Adjuvant gemcitabine plus capecitabine[74] and mFOLFIRINOX[78] both showed improved OS in phase 3 studies; neoadjuvant chemotherapy is increasingly used, with retrospective data suggesting improved survival,[84] but lack of strong evidence precludes routine use	Consider mFOLFIRINOX only for patients with ECOG performance status of 0 or 1; if preoperative chemotherapy is given, total duration of chemotherapy should be 6 months; advise clinical trial enrolment
Borderline resectable	Same as for resectable	Subgroup analysis from PREOPANC-1 study showed improved survival with preoperative chemotherapy and chemoradiotherapy[85]	Same as for resectable
Locally advanced	Systemic chemotherapy → surgical resection for down-staged patients	Multiple phase 2 and 3 studies of first-line systemic chemotherapy for locally advanced disease show benefit of induction chemotherapy[86]	For non-operative patients not progressing on chemotherapy, consider consolidative chemoradiotherapy or treatment break; no OS benefit found for chemoradiotherapy in this setting;[91] advise clinical trial enrolment
Metastatic	Systemic chemotherapy	FOLFIRINOX[92] or gemcitabine plus nab-paclitaxel[93] as first-line regimens in phase 3 studies showed improved OS when compared to gemcitabine alone	Consider FOLFIRINOX only for patients with ECOG performance status of 0 or 1; supportive care is a crucial component of management of advanced pancreatic cancer; advise clinical trial enrolment

mFOLFIRINOX=modified FOLFIRINOX (5-fluorouracil, folinic acid [leucovorin], irinotecan, and oxaliplatin). OS=overall survival. ECOG=Eastern Cooperative Oncology Group.

Table 1- 1 Guidelines for pancreatic cancer treatment plan (Mizrahi et al., 2020)

The pancreaticoduodenectomy will be applied to the tumor located at the pancreatic head (Figure 1-4). This surgery, also known as the Whipple procedure, will remove the pancreatic head, duodenum, proximal jejunum, common bile duct, gall bladder, and a segment of the stomach (Mizrahi et al., 2020). Patients will be treated by combining a distal pancreatectomy and splenectomy if the tumor forms in the pancreatic body or tail (Croome, 2014). Until 2019, there

were different studies that compared the disease-free survival time length after surgery between adjuvant gemcitabine monotherapy with different combination therapy. As shown in Table 1-1, it could conclude that the recommended therapy for patients after resection of pancreatic tumor is six months of adjuvant mFOLFIRINOX (Conroy, 2018; Tempero et al., 2019). Besides, the analysis results suggested that the treatment should initiate the adjuvant chemotherapy therapy between 28 and 59 days after surgical resection, which showed a better survival rate (Ma et al., 2019).

Surgical resection must be precluded from the treatment since extensive vascular involvement in the locally advanced pancreatic adenocarcinoma. The treatment for this group of patients would be systemic chemotherapy primarily. LAP07 trial reported that chemoradiation did not contribute to patient survival compared with systemic chemotherapy, even though it could improve the local control (Hammel, 2016). Although a small minority of these patients with an excellent response to chemotherapy might become eligible for surgical resection, the vast majority have incurable diseases. The median survival of locally advanced pancreatic adenocarcinoma ranges from 8 to 12 months (Marthey, 2015). Around half of pancreatic cancer patients are diagnosed with distant metastases. For these group of patients, systemic chemotherapy remains the primary treatment (Table 1-1), using FOLFIRINOX, gemcitabine plus nab-paclitaxel, with the purpose of palliating cancer-related symptoms and prolonging life (Conroy, 2011). The only novel therapy with a high survival rate for metastatic pancreatic cancer is the combination of fluorouracil and leucovorin with nanoliposomal irinotecan (Wang-Gillam, 2016).

Currently, the number of pancreatic cancer patients has been increasing, while the survival rate of pancreatic cancer is falling behind most major cancers (prostate, breast,

colorectal, and lung cancers). This disease remains aggressive and devastating with a dismal prognosis with slow research and clinical progress, which is in deadly need of novel diagnostic and therapeutic approaches.

1.7 Femtosecond time-resolved laser spectroscopy (fs-TRLS) technique

Dr. Ahmed Zewail's fundamentally contributed to developing the femtosecond (1fs=10-15 second) time-resolved laser spectroscopy (fs-TRLS) technique to study the transition states of chemical reactions. His work was acknowledged by the Nobel Prize in Chemistry in 1999 (Zewail, 2000), a direct and consequential technique to visualize molecular-sized reactions.

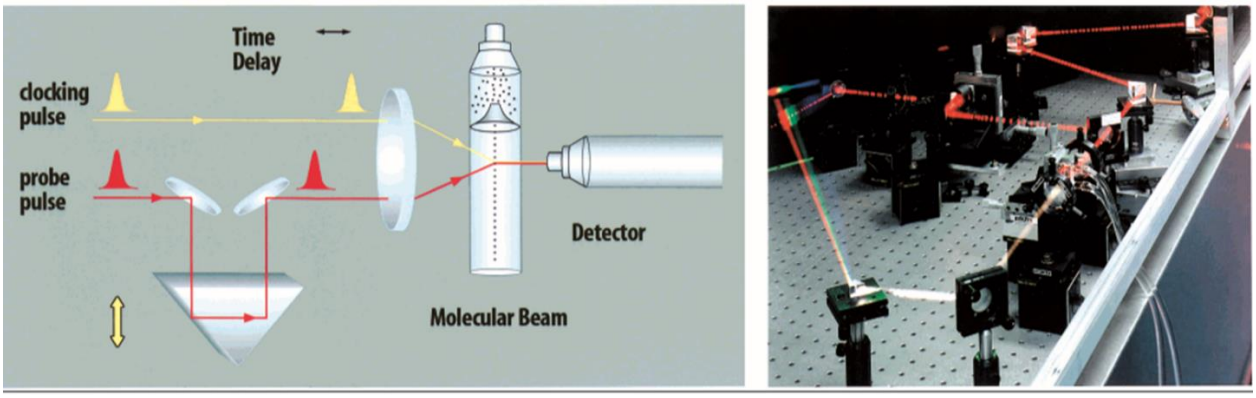

Figure 1- 6 The principle scheme of fs-TRLS technique, and an example of femtochemistry apparatus (Zewail, 2000).

As shown in Figure 1-6, the pump-probe configuration is designed to reach the femtosecond control. The femtosecond laser pump and probe pulses are generated in synchronization. The two pulses have the same finite speed (light speed), and the probe pulse is redirected through an adjustable optical path length (Zewail, 2000). The delayed arrival time

between probe pulse and pump pulse is controlled to femtosecond time resolution, making it possible to identify atomic motions in chemical reaction's transition states.

This technique has been widely used in the study of chemical processes, from bond-breaking in diatomic molecules to dynamics in larger organic and biological molecules (Stolow et al., 2004). It gives rise to femtobiology and femtochemistry, which aided the identification of the exact molecular mechanism of the clinically utilized anti-cancer medication cisplatin.

1.8 Cisplatin working mechanism – the DET reaction.

Cisplatin is a platinum chemotherapeutic medication that has been used for more than 50 years to treat a variety of human cancers (Zhang et al., 2010). The emergence of cis- [Pt (II)(NH3)2Cl2] as an anti-cancer medication ushered in a new era in cancer therapy (Chen et al., 2009). Many patients with various kinds of cancer, such as sarcoma, soft tissue, bone, muscle, and blood vessel cancers, have been effectively treated, attributable to the therapeutic usage of cisplatin (Chen et al., 2009). On the other hand, the degree of cisplatin nephrotoxicity is linked to the amount of platinum present in the kidneys (platinum concentration in the kidneys) (Nepomuceno, 2011). Platinum has serious side effects, including nausea and vomiting, decreased blood cell and platelet formation in the bone marrow (myelosuppression), hair drop, loss of hearing, and a reduced reaction to infection (immunosuppression) (Florea et al., 2011). Due to severe side effects and drug resistance, cisplatin's broad therapeutic uses have been limited in the clinic.

Understanding the mechanism of cisplatin-based chemotherapy was a significant step forward in cancer treatment research, allowing for improved efficiency and less toxic

chemotherapy medicines. Dr. Qing-Bin Lu applied femtosecond time-resolved spectroscopic techniques to determine the precise molecular mechanism of cisplatin and successfully found that dissociative electron transfer (DET) reaction with presolvated electron (e_{pre}^-) is the functioning mechanism of cisplatin (Lu, 2007).

$$e_{pre}^- + Pt(NH_3)_2Cl_2 \rightarrow [Pt(NH_3)_2Cl_2]^{*-} \rightarrow Cl^- + Pt(NH_3)_2Cl^{\bullet}$$
$$e_{pre}^- + Pt(NH_3)_2Cl \rightarrow [Pt(NH_3)_2Cl_2]^{*-} \rightarrow Cl^- + Pt(NH_3)_2^{\bullet}.$$

Figure 1- 7. The process of dissociative electron transfer (DET) reaction of Cisplatin mechanism (Lu, 2007; Lu et al., 2007)

The resultant cis-Pt (NH3)2Cl•and cis-Pt (NH3)2• radical would then lead to chemical bond break by cross bind with the guanine base (Figure 1-8), which could cause the strand breaks in DNA and then lead to the cancer cell death (Lu, 2007; Lu et al., 2007).

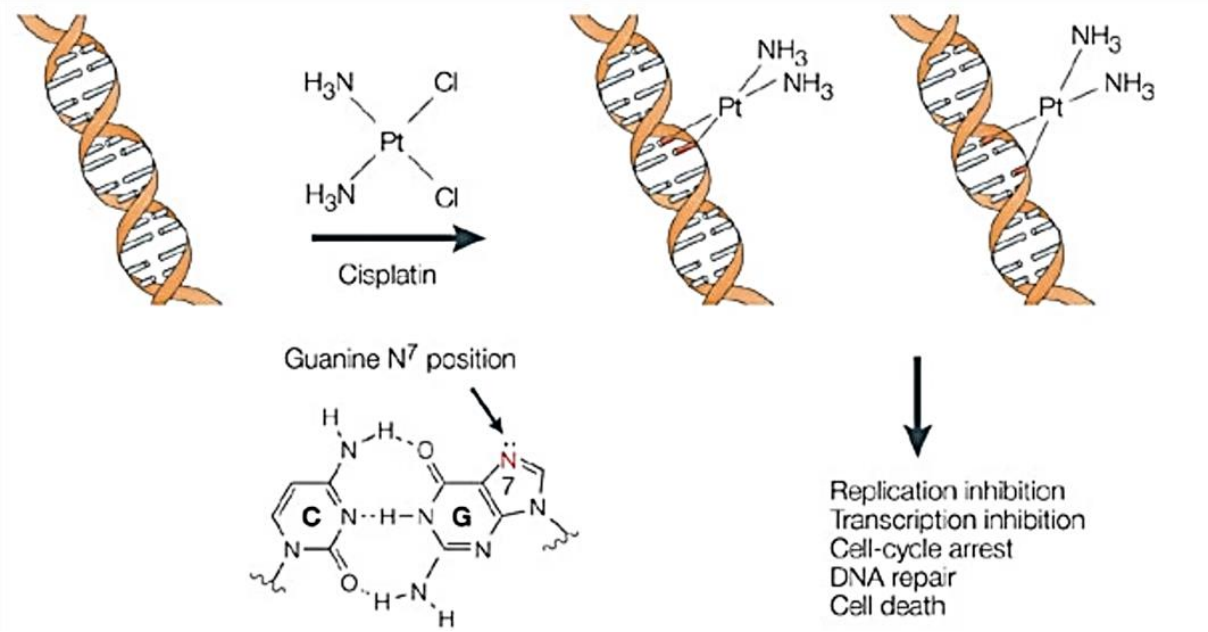

Figure 1- 8 The platinum atom in cisplatin forms covalent bonds with the N7 position of Guanine, resulting in the formation of intrastrand crosslinks of 1,2 or 1,3 strands. Different cellular responses, including replication arrest, transcription inhibition, cell-cycle arrest, DNA repair, and apoptosis, are induced by cisplatin–DNA adducts in various ways (Wang & Lippard, 2005).

1.9 The development of Femtomedicine

According to the molecular DET mechanism of cisplatin, Dr. Lu identified a series of non-platinum-based halogenated molecules (called FMD compounds) to replace cisplatin, which contains no Pt and therefore avoids the high toxicity associated with Pt. The main difference between the structure of FMD compounds and cisplatin is that an aromatic ring, instead of platinum, surround by NH2 groups and halogen atoms (Lu et al., 2015).

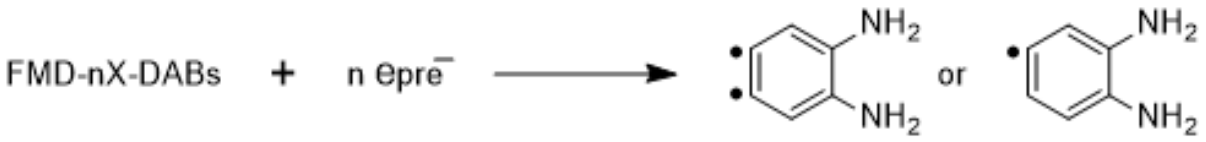

Figure 1- 9 The process of DET reaction of the halogenated molecule (FMD-nX-DABs), X refer to I, Cl, Br, and n =1 or 2

With a similar functioning mechanism, the FMD compounds (FMD-nX-DABs) are effective in DET (dissociative-electron-transfer) reaction with weakly-bound electrons (prehydrated electrons, e_{pre}-), which exist in tumor cell/tissues or exogenously produced by ionizing radiation of biological system (Lu et al., 2015).

The resulting radical of DET reaction, [B(NH2)2Xn-1] •, may substantially cause DNA damage (Lu et al., 2015), double-strand breaks that cannot be repaired spontaneously, and eventually apoptosis in cancer cells. FMD molecules are relatively non-toxic to normal cells due to the absence of heavy metals, which are the primary source of cisplatin's toxicity. These FMDs are highly effective as antitumor agents for natural targeted chemotherapy and radiotherapy of cervical, breast, ovarian, head/neck, and lung cancers with minimal side effects, which have been subsequently confirmed by in vitro/in vivo evaluation in the further research of Dr. Lu' group (Lu et al., 2015). Moreover, the previously published in vitro toxicity test result shows that the treatment of FMD compounds causes less than 5% (1/20) toxicity of cisplatin, based on the IC50 values measured by MTT assay to human normal cells (Lu et al., 2015).

Dr. Lu's research concentrated on integrating this cutting-edge technology with molecular and cell biology to enhance basic knowledge and treatment of important human diseases, most notably cancer (Lu, 2010). Based on this unique approach, he created a drug development

program based on molecular mechanisms, which resulted in the identification of novel cancer treatments (Luo et al., 2012; Lu et al., 2015; Wang et al.,2016; Goetze et al., 2019; Zhang, Q. & Lu, Q. B. 2021). This new field of femtomedicine (FMD) can improve our understanding of tumorigenesis and develop innovative cancer treatments. This FMD strategy can help save resources and expedite the process of clinical trials and treatment.

1.10 Chemotherapeutic effect of FMD agent on pancreatic cancer

As discussed above, pancreatic cancer is a disease in desperate need of new therapeutics. This project investigated one of the FMD compounds, 1,2-Diamino-4,5-dibromobenzene (FMD-2Br-DAB), to in vitro evaluate the therapeutic efficacy for pancreatic cancer. The structure and the functioning mechanism of the investigated FMD agent, FMD-2Br-DAB, are shown in Figure 1-10. The produced reactive radical of DET reaction will mainly induce DNA damage in cancer cells (Lu et al., 2015)

Figure 1- 10 The molecular structure of FMD-2Br-DAB and complete process of its DET reaction.

Prior to this thesis work, our collaborators in University Medicine Goettingen, Germany, had performed a pilot study of FMD-2Br-DAB in genetically engineered mouse models of pancreatic cancer, which is highly resistant to standard chemo- and radiotherapy (Goetze et al. 2019). The results showed that the FMD significantly reduced cell viability in some pancreatic cancer cell lines and tumor frequency in KC mice, exhibiting a preventive role of the FMD

against tumors, and the FMD at 7 mg/kg (i.p.) had comparable therapeutic effects to the current clinically used gemcitabine at 100 mg/kg (i.p.) in the KPC mouse model (Goetze et al., 2019). The study in Germany also confirmed the radio-sensitizing effect of the FMD in combination with X-ray radiation (Goetze et al., 2019). However, much information in preclinical evaluation of the FMD for treating pancreatic cancer is needed, especially on the well-controlled in vitro experiments and the potentiality to overcome the drug resistance, the major obstacle in clinical oncology.

As further FMD drug evaluation studies to pancreatic cancer, this project will perform four different kinds of in vitro assay of the anti-tumor effect of FMD agent and the toxicity level to human health, including MTT assay, clonogenic assay, DNA double-strand break measurement, and Caspase3/7 detection. These measurement approaches evaluate the different characteristics of the FMD agent from the aspect of cytotoxicity, cell reproductive ability damage, DNA damage ability, and induction of cell apoptosis.

This well-defined cell-based in vitro assays will be introduced, and the results will be presented and discussed in later Chapters.

Chapter 2 Examination of cell viability of human normal cells and pancreatic cancer cells with MTT assay after the FMD treatment

Cell-based assays are commonly utilized for screening assortments of mixtures to decide whether the test particles have impacts on cell multiplication or show direct cytotoxic impacts that will ultimately lead to cell death (Riss et al., 2016). This chapter describes MTT assay, one of the most commonly cell-based assays, which is used to examine the cytotoxicity of compounds or testing cell metabolic activity in multi-well plates. The results of the MTT assay effectively indicated the anti-cancer efficacy and cytotoxicity of FMD compounds to PANC-1 / BxPC-3/ L 3.6 / GM05757 cell lines.

2.1 Introduction of MTT assay

In cell culture, MTT assay is firstly introduced by Mosmann as a high-throughput screening approach in 96-well plates (Mosmann, 1983). MTT (3-(4,5-dimethylthiazol-2-yl)-2,5-diphenyltetrazolium bromide) assay is a colorimetric assay using the tetrazolium salt thiazolyl blue (Mosmann, 1983), which are widely applied in studies of cell biology for assessment of cytotoxicity, cell viability, and proliferation.

MTT assay is one of the most effective methods to check cell lines' cell viability and evaluate the safe and efficient amount of the drug. (Stockert, 2012). Because of the positive net charge and lipophilic side groups (Figure 2-1), the MTT compound can pass the cell layer and is diminished in reasonable cells by mitochondrial or cell plasma proteins like oxidoreductases, dehydrogenases, oxidases, and peroxidases utilizing NADH, NADPH, succinate, or pyruvate as

an electron giver. This outcome in a transformation of MTT to the water-insoluble formazan (Figure 2-1) (Berridge et al., 2005).

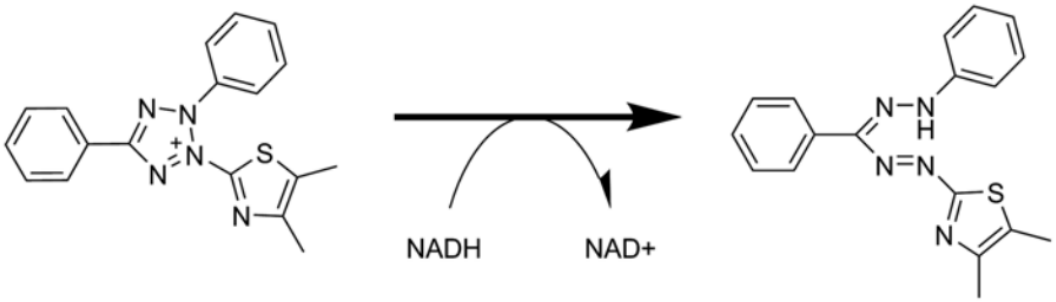

Figure 2- 1. Enzymatic reduction of MTT to formazan. Formazan forms solid crystals that pierce the cell's membrane.

Aside from enzymatic processes, there are many nonenzymatic interactions with reducing molecules such as coenzyme A, glutathione, or ascorbic acid, that can interact with MTT and form the formazan product having a greater absorbance (Riss et al., 2016). The production of needle-like formazan crystals breaks the integrity of the cell, resulting in cell death. As a result of the breakdown in metabolism, the MTT to formazan conversion is disrupted quickly. MTT assay is known as an endpoint determination because of the cell death-associated reaction halt. MTT-based test procedures usually include a cell lysis phase and a formazan-dissolving step for the intracellularly generated crystals before a spectroscopic measurement. Based on Mosmann's findings, subsequent research provided various adjustments to increase the assay's performance and sensitivity, but the difficulty of dissolving solid formazan crystals remained (Hansen et al., 1989).

2.2 Procedures of MTT assay

In order to prepare the MTT stock solution, 500 mg MTT powder (Sigma, St. Louis, USA) are dissolved in 10 mL (PBS) phosphate buffer solution by stirring the solution with a magnetic stirrer for about 1 hour avoid light, to sterilize the solution using a 0.22 mm filter, then store it in 1-mL aliquots (50 mg/mL) under -20°C (Van Meerloo et al., 2011). Before use, the stock solution will be diluted with PBS 10 times to (5 mg/mL).

3000-5000 cells/well were seeded in a 96-well flat-bottom microtiter plate (BD Falcon™, Corning Inc., NY, USA) and incubated for 24 hours in a 5% CO2 incubator at 37°C for cells to adhere. After 24 hours, the culture medium was withdrawn from each well; then, cell samples were treated with various concentrations of the designed compound in the complete cell culture medium for 48 hours at 37°C in a 5% CO2 incubator. After two days of incubation, the cell culture medium was replaced with 100 µL transparent complete cell culture medium (without phenol red). Subsequently, 10 µL of MTT working solution was added to each well. After the plate was incubated for 4 hours, the formed formazan crystals were solubilized by adding 100 uL solubilizing SDS-HCl solution (10% SDS in 0.01 M HCl) per well for 4-5 hours at 37°C in a humidified 5% CO2 atmosphere. Finally, the optical density of the dissolved formazan crystals (purple color) was measured at absorbance 570 nm using the Multiscan GO microplate spectrophotometer (Thermo Scientific, Mississauga, ON, Canada). The schematic process of the MTT assay has been given in Figure 2-1 (Bahuguna et al., 2017).

For each group of all different treatment concentrations, five replicates were set for all MTT experiments, and the error bars indicated the standard deviations of the replicates. The untreated (control) cells were used to represent cell viability, and the blank control wells without cells were used to assess unspecific formazan conversion.

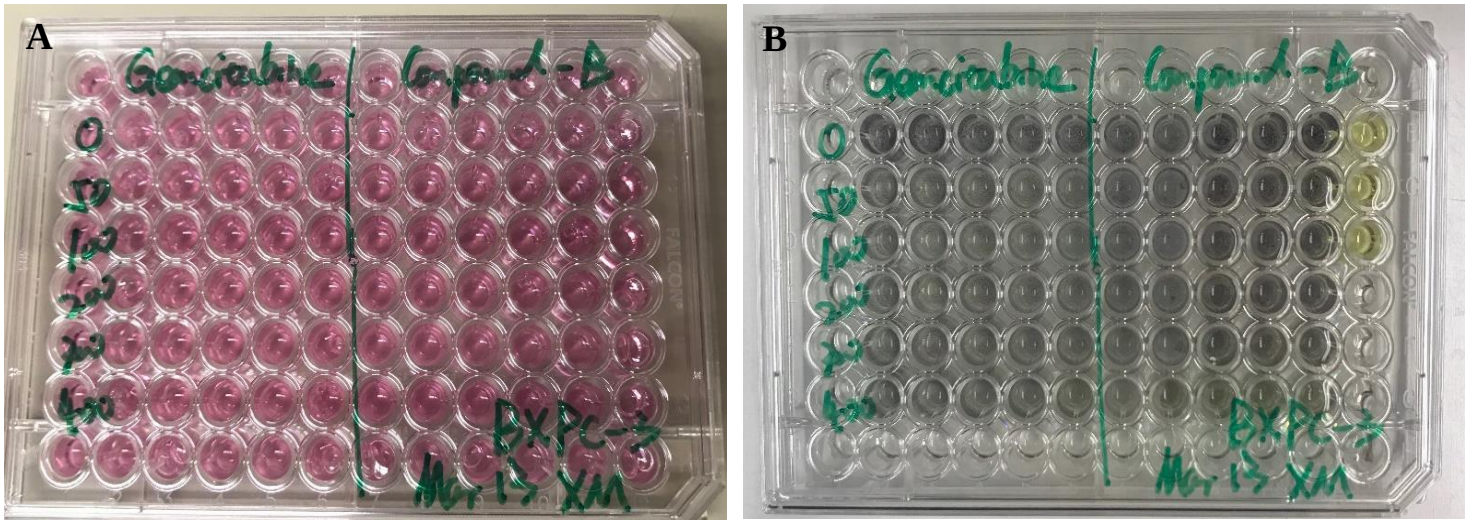

Figure 2- 2 MTT assay performance in a 96-well flat-bottom plate testing viability of adhered cell lines (BxPC-3 cell line). (A) 96-well plate after various concentrations of the designed compound are added in each well. (B) 96-well plate after produced formazan crystals dissolved in SDS-HCl solution (before optical density measured).

2.3 Cytotoxicity & Anti-Cancer Effect Tests of FMD by MTT assay

2.3.1 Cell lines

Three representative human pancreatic cancer cell lines (BxPC-3/PANC-1/ L3.6, ATCC) were investigated in this project for their differences in cell morphology, cell motility, and various metastasis potentials (Figure 2-3). The BxPC-3 cell line was cultured from the locally advanced tumor (no metastasis), and this cell line produces human pancreatic cancer-associated antigen and carcinoembryonic antigen in the mouse model (Tan et al.,1986; Deer et al., 2010). As metastatic cancer cells, the motility of PANC-1 cells was proven experimentally to be five-fold higher than the motility of BxPC-3 cells (Deer et al., 2010). Furthermore, as shown in Figures 2-3-A and 2-3-C, PANC-1 cells seemed to move mainly as single cells, whereas BxPC-3 cells looked to travel as a densely packed sheet, indicating that PANC-1 cells were more likely to migrate as single cells. In culture, the PANC-1 cell line did not produce any notable carcinoembryonic antigen (Lieber et al.,1975). Besides, L3.6 is also a highly metastatic human pancreatic cell line that has been utilized to investigate the mechanisms of antitumor activity induced by various chemotherapeutic drug combinations, including chemotherapy alone (Vincent et al., 2011). These cell lines are appropriate for the suggested investigation.

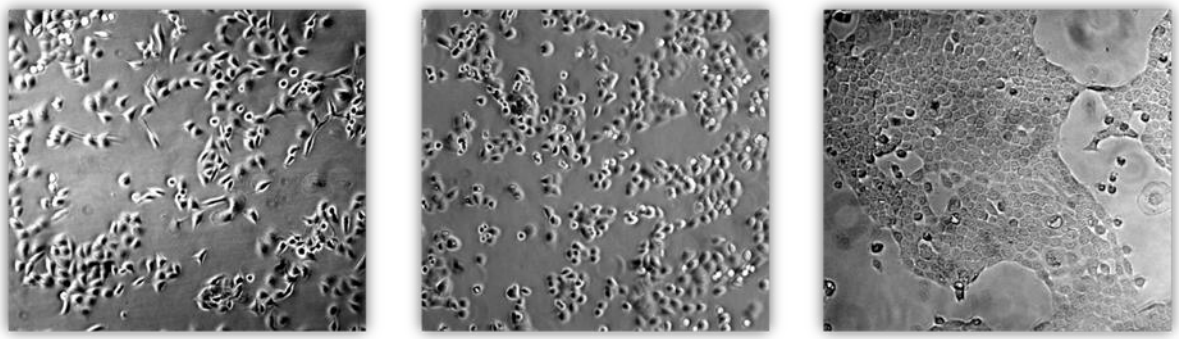

Figure 2- 3. Micrographs of the three kinds of pancreatic cancer cells. A: PANC-1 pancreatic cancer cell line; B: L3.6 pancreatic cancer cell line C: BxPC-3 pancreatic cancer cell line

In the whole culturing process, these three pancreatic cancer cell lines were cultured in T25 flasks at 37 ºC with 5% carbon dioxide in the water-contained incubator. The base medium is Dulbecco's Modified Eagle's Medium for PANC-1 and L3.6 cell lines, and RPMI-1640 Medium for BxPC-3 cell line is. In order to complete the growth medium, the base medium is supplemented with 10% Fetal Bovine Serum. In order to eliminate any potential contamination, the complete growth medium should include 1% of Penicillin-Streptomycin. Besides, the complete growth mediums of BxPC-3 and L3.6 are contained 1% 200 mM L-Glutamine (final concentration is 2mM).

The human skin diploid fibroblast cell line (GM05757) is applied to test the possible harm of drugs to human health, which is very susceptible to exogenous chemical toxicity (Lu et al., 2013). GM05757 cell line was cultured with MEM supplemented with 10% fetal bovine serum (FBS), 100 units/mL penicillin G, and 100 mg/mL streptomycin (Hyclone). All three pancreatic cancer cell and human skin normal lines are stored in the liquid nitrogen vapor phase.

Before the main therapeutic tests, unfreeze cancer cells were passaged more than once to ensure high cell activity.

2.3.2 In Vitro MTT Results Between Pancreatic Cancer Cells and Normal Cells

The in vitro anti-tumor effects and cytotoxicity of FMD compound were investigated in normal human skin diploid fibroblast cell line (GM05757) and three human pancreatic cancer cell lines (BxPC-3; PANC-1; L3.6). The cells were treated with different concentrations of FMD compound and incubate for 48 hrs, and then the cell viability in each group was tested by MTT assay. According to the optimal reaction of cell lines' metabolic activity to the tested drugs, MTT assay is designed to perform with 0 to 300 μM of FMD compound. .

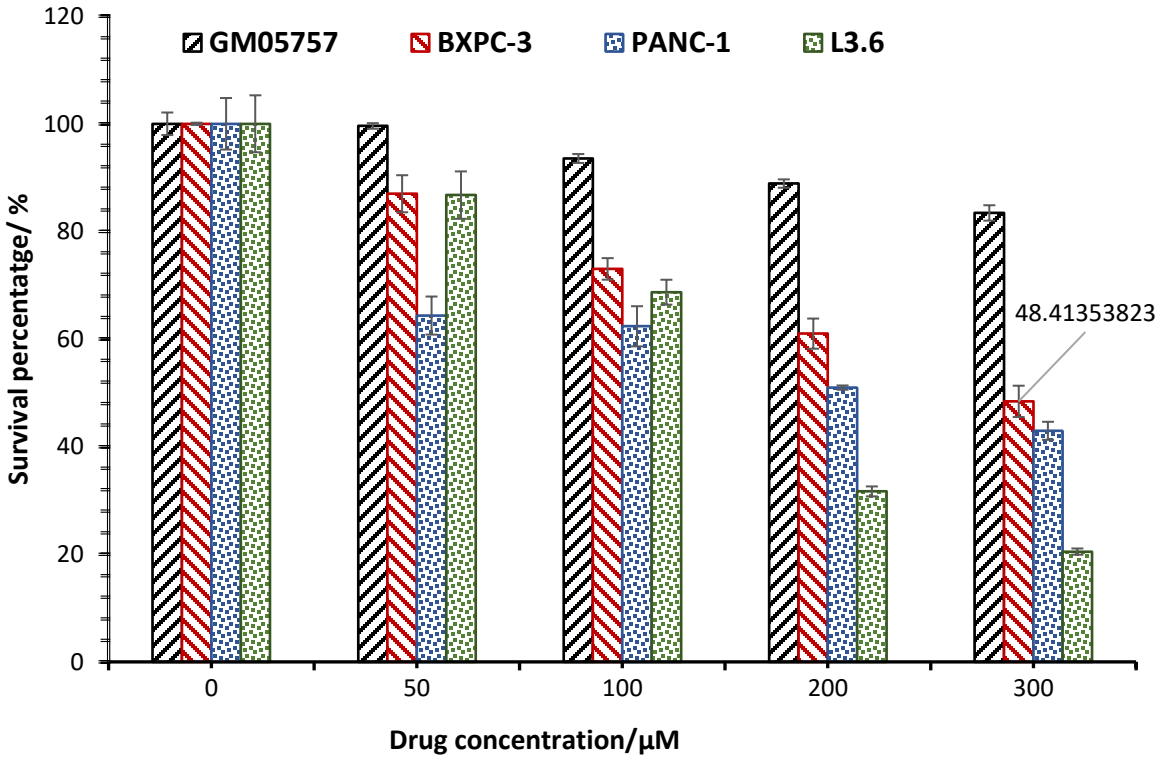

Figure 2- 4 Cytotoxicity & Anti-Cancer Effect test of FMD compound: 4 cell lines' viability tested by MTT assay (treated 48 hours)

Figure 2-4 shows that the normal GM05757 cells were the least susceptible to the FMD compound treatment, indicating that they were not sensitive to the FMD compound. In contrast, the cell viability of three pancreatic cancer cells keeps decreasing with higher doses of FMD compound. The survival rate of the three cancer cells dropped over 50% by 300 μM of FMD compound. Thus, the FMD compound exhibited a strong antitumor effect in this MTT cell viability result, demonstrating that the FMD agent selectively killed more pancreatic cancer cells than normal cells compared to normal human cells.

2.3.3. In Vitro MTT Toxicity of Human Normal Cell, FMD VS Clinic Drug.

Normal human skin diploid fibroblast cell line (GM05757) was treated with different concentrations of FMD or Gemcitabine (mentioned in chapter 1, an important clinically using chemotherapy drug for pancreatic patients) for 48 hrs.

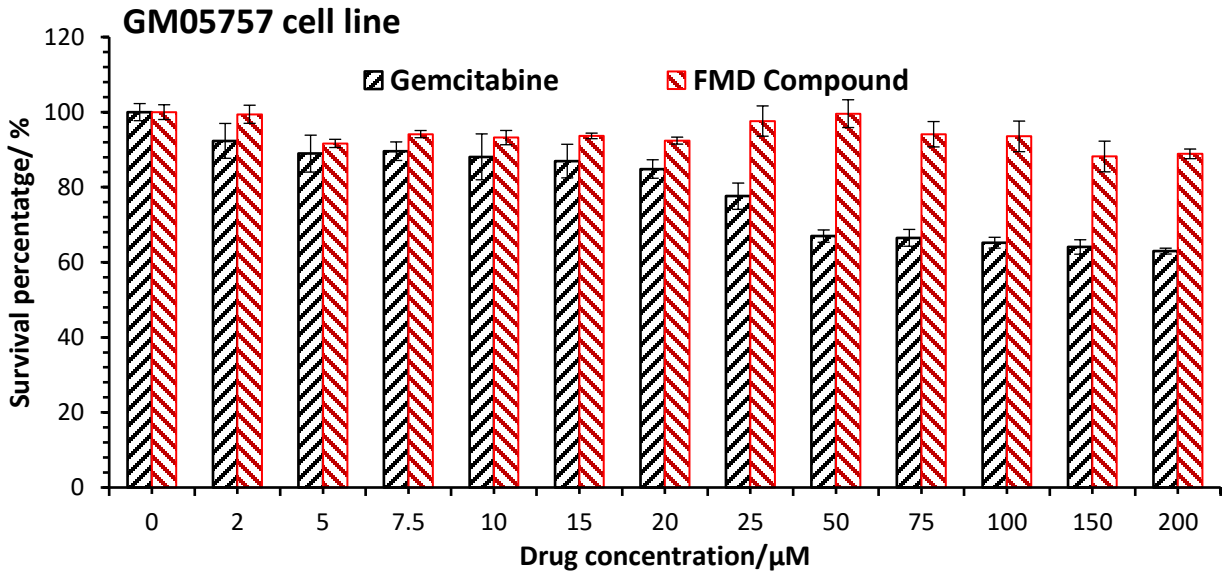

Figure 2- 5 Comparison cytotoxicity of FMD and clinic drug to GM05757 by MTT assay (48hrs)

As shown in Figure 2-5, the viability of GM05757 (normal cell) decreases while the Gemcitabine concentration increases. This figure indicates that Gemcitabine is more toxic than the FMD compound, especially at high concentrations, which significantly induced more normal cell death. In contrast, the increasing concentration of FMD compound does not appear high level of toxicity for human normal cells.

The findings of this MTT test demonstrate that Gemcitabine is much more hazardous to human normal skin cells than FMD compound, where the cytotoxicity of FMD to human normal skin cell line is less than 20%.

2.3.4. In Vitro Anti-Cancer Effect MTT Tests, FMD VS Clinic drug

The in vitro anti-tumor effects of FMD agent were investigated in human pancreatic cancer cell lines, comparing with the therapeutic effect of clinical drug Gemcitabine. The human pancreatic cancer cell line (PANC-1) was treated with varying concentrations of FMD or Gemcitabine for 48 hours before being tested using the MTT method, and additional low-dose groups were performed.

The findings of this MTT experiment demonstrate that the PANC-1 cell line has a dose-dependent manner with low concentrations ($\leq$ 50μM) of Gemcitabine. For high doses, the PANC-1 cell line exhibited resistance to this clinically used medication. In contrast, the FMD compound increasingly killed PANC-1 pancreatic cancer cells efficiently proportionally depending on the doses.

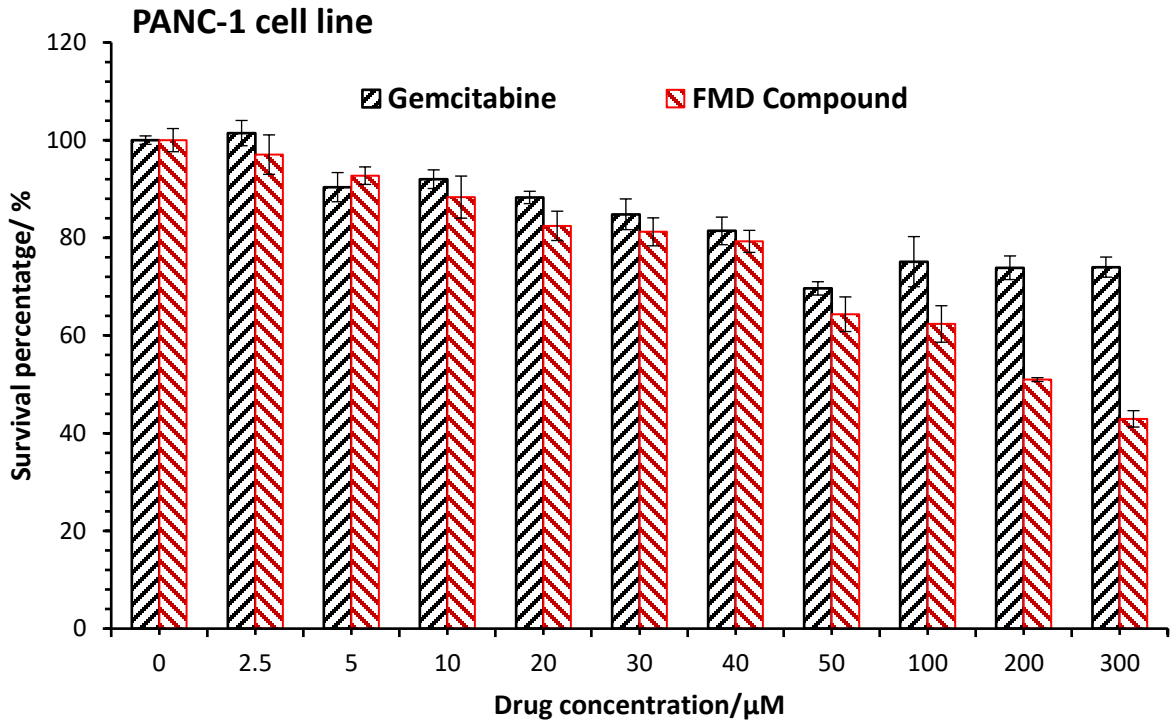

Figure 2- 6 FMD therapeutic effect to PANC-1 comparison with clinic drug by MTT assay (48hr)

BxPC-3 pancreatic cancer cell line are selected to process in vitro anti-cancer effect tests with MTT assay. FMD or Gemcitabine treated the cell line for 48 hours, and the drug concentration gradient was designed from low to high doses. The MTT result is demonstrated below.

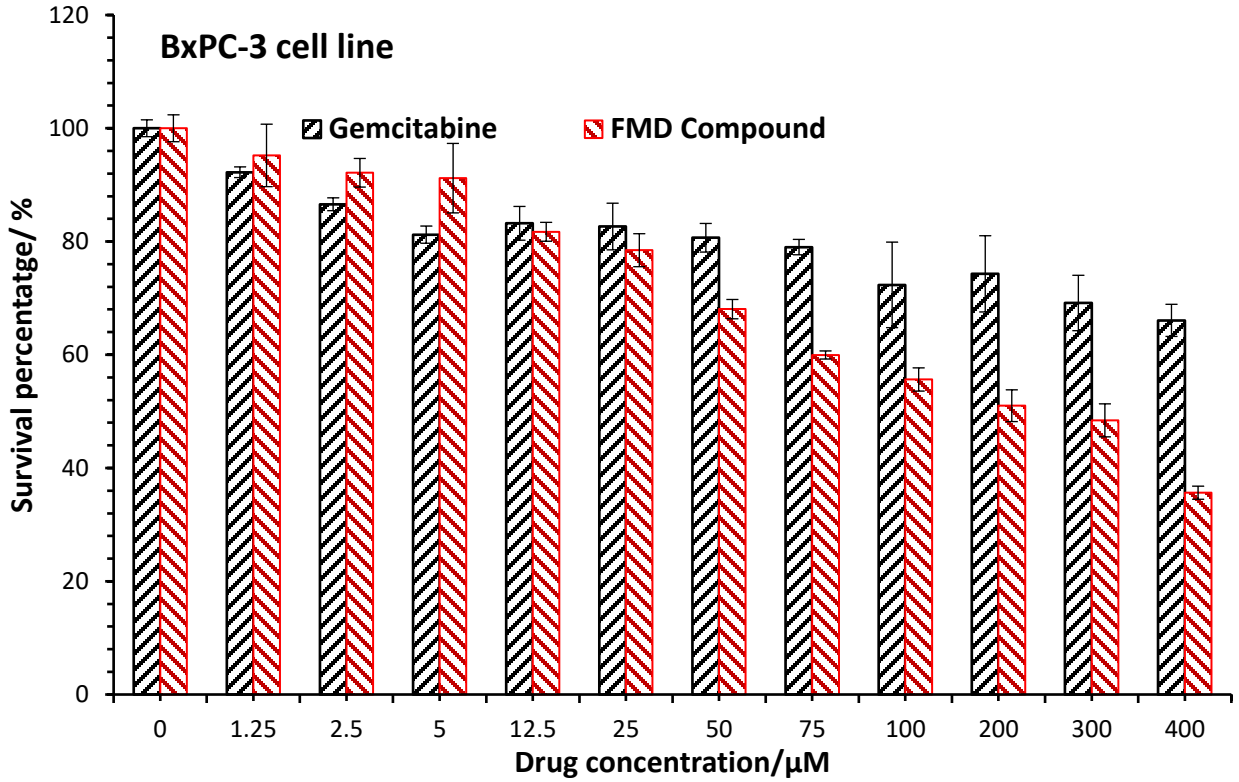

Figure 2- 7 FMD therapeutic effect to BxPC-3 comparison with clinic drug by MTT assay (48hr)

MTT test result indicates that the percentage of BxPC-3 cells killed by Gemcitabine depends on its increasing concentration at the low range. At the high concentrations, the treatment efficiency of Gemcitabine was only slowly enhanced with more doses. Compared with the Gemcitabine group, compound FMD compound killed BxPC-3 pancreatic cancer cells more efficiently as the drug concentration ≥50 μM (not ≥25 μM, considering the experimental error).

The L3.6 cell line is also investigated for in vitro anti-cancer effect tests with MTT assay. The following figure shows that this cell line is treated with a concentration gradient by the FMD agent or Gemcitabine for 48 hours.

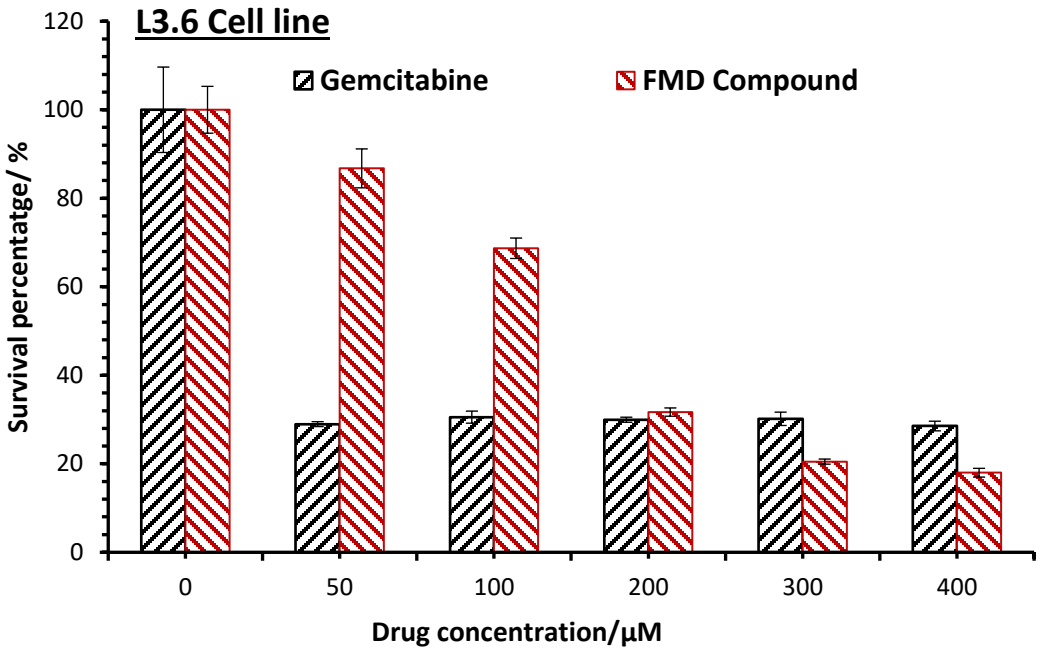

Figure 2- 8 FMD therapeutic effect to L 3.6 cell line comparison with clinic drug by MTT assay (48hr)

When seen in Figure 2-8, the gemcitabine could kill about 70% of L3.6 cells at low concentrations, and the medication's impact remained constant as the concentration of the drug was increased. On the other hand, FMD Compound has more outstanding results when used at more significant concentrations (over 200 uM).

It can be shown that the L3.6 pancreatic cancer cell exhibits resistance to Gemcitabine at concentrations ≥ 50 μM, which indicates that this clinically utilized medication could not wholly kill L3.6 cells even with a considerable dose. It is consistent with the drug's resistance performance in the clinic for late-stage patients who usually require long-term chemotherapy treatment. In contrast, the FMD compound has better treatment performance at more significant concentrations, and it may be feasible to eradicate all L3.6 cancer cells after repeated treatments in the long term.

2.4 Conclusion from the MTT Results

With the MTT assay, the in vitro anti-tumor effects of FMD were evaluated with human normal skin cell line (GM05757) and three human pancreatic cancer cell lines (BxPC-3; PANC-1; L3.6). The results show that the FMD compound could effectively kill pancreatic cancer cells without any significant influence on the cell viability of Normal GM05757 cells. It is observed that pancreatic cancer cells developed drug resistance to Gemcitabine (clinically used medication for pancreatic cancer) at concentrations $\geq$ 50 μM. In contrast, the FMD compound's therapeutic effect on pancreatic cancer cells improved with increasing drug doses, exhibiting a dose dependence of the antitumor efficacy. It is confirmed that the FMD compound is a potent anti-tumor agent targeting pancreatic cancer cells in the clinic.

Chapter 3 Determination cell reproductive ability damage of FMD in pancreatic cancer by clonogenic assay

The clonogenic assay (colony formation assay) has become the most well-accepted approach for determining cell reproductive ability in medical biology research. It is frequently used to evaluate the effectiveness of other cytotoxic drugs on various cell lines (Franken et al., 2006). Furthermore, the clonogenic assay is often used to assess the impact of cytotoxic drugs and other anti-cancer treatments on colony-forming abilities in cell lines of varying sensitivity (Rafehi et al., 2011). This chapter will introduce and summary the result of applying the clonogenic assay to determine the cytotoxicity of designed compounds from cell reproductive ability after treatment. The clonogenic assay results effectively illustrated the therapeutic efficacy and cytotoxicity of the Femto-medicine compound to PANC-1/ BxPC-3/ GM05757 cell lines (pancreatic cancer cell lines and human skin normal cell line).

3.1 Introduction of clonogenic assay

The clonogenic (or colony-forming) assay has been in use for over 50 years, the first article detailing the procedure being published in 1956, tested with mammalian (HeLa) cells in culture (Puck & Marcus, 1956). Currently, the clonogenic assay is widely employed in cancer research since the production of clones is thought to represent the feature of cancer cells with tumor-initiating capacities. While this assay originated in the field of radiobiology, it has now evolved into a standard tool in cancer research for assessing cellular proliferation and the cytotoxic effects of numerous medicines with therapeutic potential. On their own or in combination, this comprises chemotherapeutic medicines and targeted therapy (Munshi, Hobbs & Meyn, 2005).

Various conditions cause cell death, but the most frequent characteristics are losing reproductive integrity and the inability to proliferate indefinitely. As a result, a cell that can generate proteins and DNA and go through one or two mitoses but cannot divide and create a large number of progenies is classified dead. Therefore, the endpoint measured with cells in culture is known as loss of reproductive integrity of reproductive death (Stoddart, 2011). The ability of a single cell to develop into a colony is visible to the naked eye, indicating it has its reproductive capability (Munshi, Hobbs & Meyn, 2005). The dosage-survival curve describes how this capacity deteriorates as a function dose of chemotherapy or radiation treatment. The effects of numerous drugs, either in combination or alone, are now widely studied in most research using established cell lines.

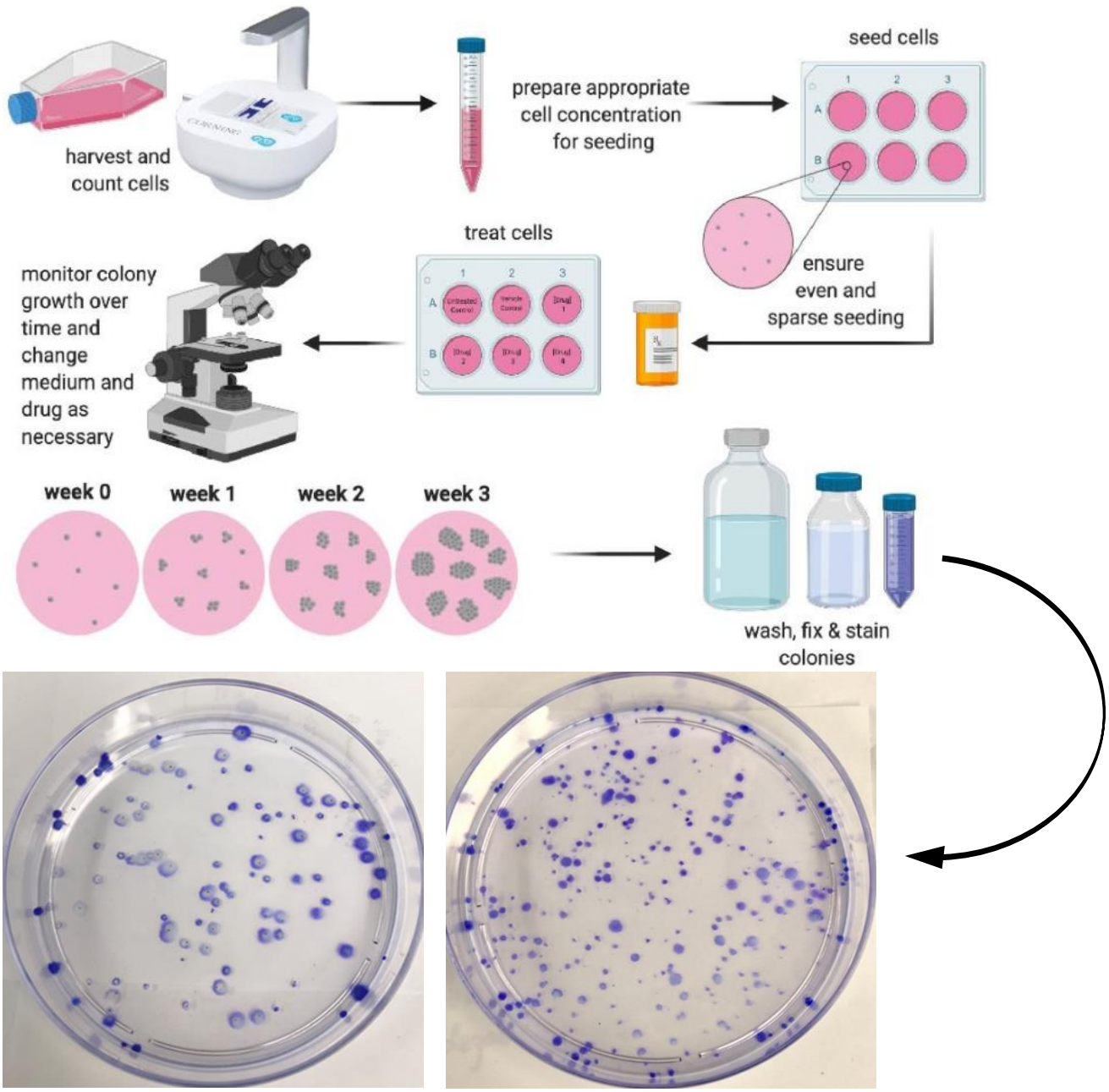

Figure 3- 1. Briefly summary clonogenic assay protocol. (A) individual cell suspension was collected by trypsinzed, prepare appropriate cell concentration for seeding in each plate (100mm) of different groups, applied different designed treatment to each group, clonogenicity assessed. (B) Two samples after the colonies were stained and counted after 14 days' 37 degree and 5% CO2 incubation.

3.2 Procedures of Clonogenic survival assay

Essentially, the clonogenic test allows researchers to compare the reproductive viability (the ability of cells to generate progeny, the ability of a single cell to form a colony of 50 or more cells) of untreated control cells against cells that have received various treatments. Every cell in the population is tested for its ability to divide indefinitely (Franken et al., 2006). Only partial of planted cells may form colonies. Cells are seeded out with appropriate dilutions before treatment in order to establish colonies in around two weeks.

Harvested cells are trypsinized to prepare single-cell suspensions by rinsing with phosphate-buffered saline and then treating with a 0.05 percent trypsin/EDTA solution for 1-2 minutes when the cells start to become rounded, and 30% of them are detached and pipetting up and down 20 times to separates the cells, centrifuging the suspension to remove trypsin (Rafehi et al., 2011). The quantity of cells in each sample is meticulously counted before being diluted and planted into Petri plates in the right quantities (five replicates of each designed group in 100 mm dishes). After (around 4 hours), cells are attached to the plate, the designed treatments are applied to each sample, then Petri dishes are placed in an incubator and kept at 37°C in a 5 percent CO2 atmosphere for colony formation (Rafehi et al., 2011). For various cell lines, the incubation time for colony formation ranges from 1-3 weeks. In this project, cell lines were treated for 48 hours and terminated by replacing fresh complete cell culture media. It takes 14 days for human pancreatic cancer cells and normal skin cell lines to generate sufficiently big clones of 50 or more cells in the control dishes. For fixation and staining of colonies, plates are washed carefully with PBS, and colonies are fixed with glutaraldehyde (6.0% v/v), stained with crystal violet (0.5% w/v) (add 2–3 ml the mixture of 6.0% glutaraldehyde and 0.5% crystal violet), leave this for at least 30 min. Then stained colonies are rinsed with tap water carefully

and leave the dishes or plates with colonies to dry in normal air at room temperature (20 degrees).

Plating efficiency (PE) is the number of colonies divided by the number of cells implanted, depending on the cell line. The surviving fraction (SF) is calculated by dividing the PE of treated cells with the PE of the controls (the equation of PE and SF are indicated below). The result of data is plotted with the treatment dosage on the x-axis and surviving fraction on the y-axis.

$$PE = \frac{No.of\ clonoies\ formed\ without\ treatment}{No.of\ cells\ seeded} * 100\% \qquad (3.1)$$

$$SF = \frac{No.of\ clonoies\ formed\ after\ treatment}{No.of\ cells\ seeded * PE} * 100\% \qquad (3.2)$$

Same as MTT assay, for each group of all different treatment concentrations, five replicates were set for all clonogenic experiments, the error bars indicated the standard deviations of the replicates, and the groups of untreated (control) cells were used to represent cell viability.

Preparation experiments are set up to determine each designed group's optimum seeding cell number for different cell lines. Each treated and untreated group is established with four different cell numbers to determine the best seeding cell number for the most colonies. The plating efficiency and survival fraction were calculated using the average colony count for the five dishes of each group in the formal set experiments.

.

3.3 Cytotoxicity & Anti-Cancer Effect Tests of FMD by clonogenic assay

3.3.1 Cell lines and preparation

Two human pancreatic cancer cell lines (BxPC-3; PANC-1) and normal human skin diploid fibroblast cell line (GM05757) are selected to test reproductive integrity and the ability to proliferate by clonogenic assay.

For the preparation of the clonogenic assay, all cell lines are stored and harvested under the same conditions as mentioned in Chapter 2 for the MTT assay. Cell samples were passaged around 2 to 3 times before performing the experiments.

3.3.2 Clonogenic Results Between Pancreatic Cancer Cells and human normal Cells

As a more sensitive cell-based measurement, the clonogenic assay's preparation experiment shows the survival fraction is close to 0 when cells are treated with ≥ 50 μM of FMD compound with the vehicle. Therefore, the drug concentration gradient is designed from 0 to 50 μM for the formal sets. . The equal treatment was given to all of the plates (100mm) for all three cell lines and terminated the treatment after 48 hours by replacing the drug solutions with fresh complete culture media. The surviving fraction is computed using the equations (3.1 and 3.2) and Figure 3-2 compares the reproductive integrity of pancreatic cancer cells to that of human normal cells after treatment.

As demonstrated in Figure 3-2, the survival fraction of pancreatic cancer cells decreases as the concentration of FMD agent increases, while the survival fraction of GM05757 decreases just slightly. FMD treatment harms the proliferative capacity of human normal cells by less than 20% at 50 μM, while FMD treatment positively affects the reproductive integrity of pancreatic cancer cells by 60-70 percent at 50 μM. Femtomedicine compound was shown to destroy more pancreatic cancer cells than normal cells preferentially. The results of this test are consistent with those of the prior MTT assay.

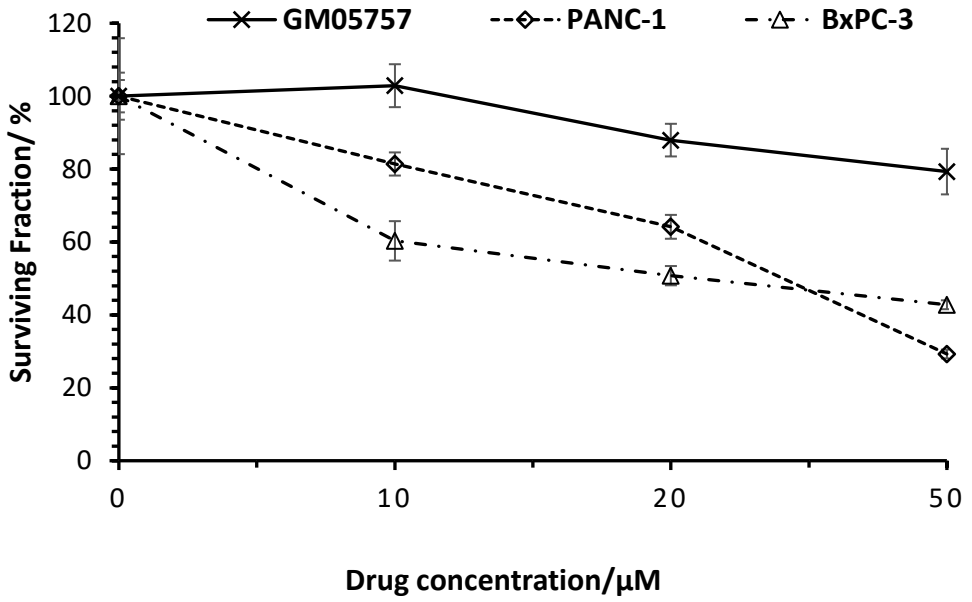

Figure 3- 2 Cytotoxicity & Anti-Cancer Effect test: 3 cell lines test by clonogenic assay treated 48 hours excluded the effect of the vehicle.

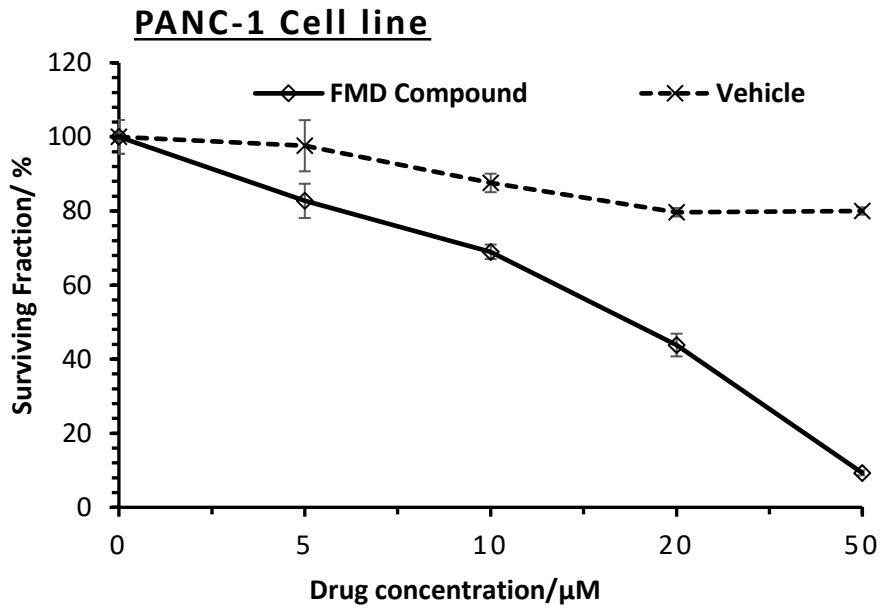

Figure 3- 3 In vitro anti-Cancer Effect test: PANC-1 test by clonogenic assay treated 48 hours. Vehicle control group: Vehicle (equal amounts of each FMD concentration gradient) was applied to the designed plates without adding any medication.

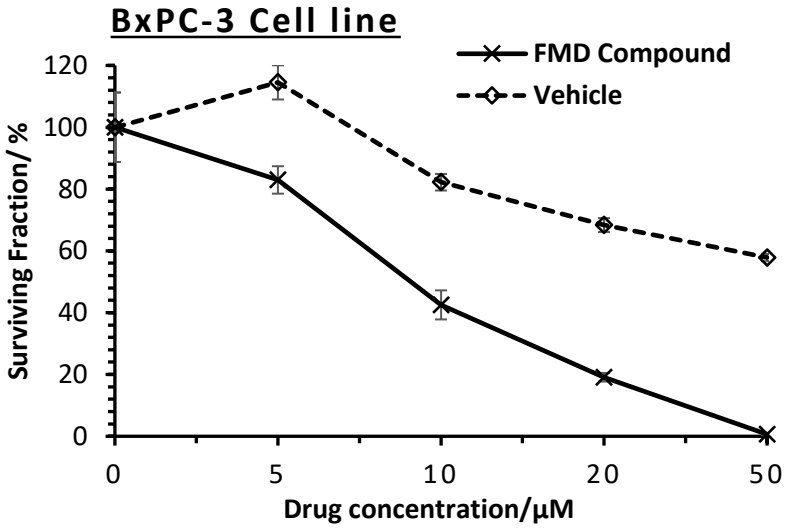

Figure 3- 4 In vitro anti-Cancer Effect test: BxPC-3 Test by clonogenic assay treated 48 hours. The vehicle control group was added to the designed plates by the same amount of each FMD concentration gradient without the drug.

The comparison between the FMD compound and vehicle to PANC-1 and BxPC-3 is shown in Figures 3-3 and 3-4. These clonogenic assay results illustrate that FMD compounds effectively reduce the colony-forming abilities of PANC-1 and BxPC-3 pancreatic cancer cells with increasing concentration. The FMD compound effectively caused pancreatic cancer cells to lose reproductive ability with or without the effect of the vehicle.

3.4 Conclusion from the Clonogenic Assay Results

This Chapter aimed to verify the effectiveness of the FMD compound from colony-forming ability after the treatment to various cells.

From the therapeutic effect evaluation by clonogenic assay, reproductive integrity and the capacity to proliferate are tested in two human pancreatic cancer cell lines (BxPC-3; PANC-1) and a normal human skin cell line (GM05757). The results in this chapter supported that the FMD compound intensifies the damage to reproductive integrity of different pancreatic cancer cell lines with higher concentrations. However, there was no significant effect by increasing the amount of FMD compound to the reproductive ability of human normal cells. It can be confirmed that FMD compound has the potential to induce the cell death to pancreatic cancer cell selectively, which prove the high potential of therapeutic effect of FMD compound to pancreatic cancer patients in the clinic.

Chapter 4 Assessment of DNA DSB in human normal cells and pancreatic cancer cells by the FMD Treatment through HCS DNA Damage Assay

The HCS (High Content Screening) DNA Damage test is extensively used as an indicator test of DNA double-strand break damage in various scientific areas, including radiation biology, clinical research, and cancer biomarker development. The in vitro HCS DNA double-strand break assay, in particular, has been proposed as a new in vitro DNA damage test with promise as a pre-screening tool (Garcia-Canton, Anadon & Meredith, 2013). The approach takes full advantage of the microscopy-based system's combination technology of cellular image acquisition with software quantification for High Content Screening (HCS), which offers the opportunity to reliably assess the effects of potential therapeutic induced genetic damage while reducing the dependence on animal models. In this chapter, the HCS DNA damage assay will be introduced and applied to determine the DNA damaging ability of designed compounds from the fluorescent intensity of dyed DNA double-strand break in cells after treatment. Both characteristics were evaluated concurrently in the same cell by combining particular antibody-based DNA damage detection with a cytotoxicity indicator. The HCS DNA damage test successfully demonstrated the inducing DNA DSB ability and cytotoxicity of Femto-medicine chemicals in PANC-1/ BxPC-3/ GM05757 cell lines (two pancreatic cancer cell lines and a human skin normal cell line).

4.1 Introduction of HCS DNA Damage Assay

The DSB (double-strand break) is one of the most severe forms of DNA damage that occur intracellularly. Exogenous factors like some chemotherapeutic medicines, ionizing radiation (IR),

endogenously produced reactive oxygen species, and mechanical stress on the chromosomes contribute to these changes (Khanna & Jackson, 2001). Even though cells may adapt to moderate levels of irreversible damage, a single DNA double-strand break (DSB) can cause apoptosis if it inactivates a vital gene (Rich, Wyllie & Allen, 2000). Because the repair of DNA DSBs is inherently more complex than that of other kinds of DNA damage, they are thought to be especially physiologically significant (Khanna & Jackson, 2001). Therefore, the double-strand break (DSB) in genomic DNA in mammalian cells is a life-threatening lesion, while one of the recognized reactions to DSB formation is phosphorylation of H2A histones. The proteins involved in DSB repair are aided by phosphorylated H2AX, which is phosphorylated in human cells by phosphatidylinositol 3-kinase-like protein kinases such as ATR (ATM- and Rad3-related) and ATM (ataxia-telangiectasia mutated) (from Figure 4-1) (Tšuiko et al., 2019). DNA damaging elements cause the histone variation H2AX (Ser139) to be phosphorylated, resulting in the formation of DNA foci at the location of DNA DSBs (Figure 4-1).

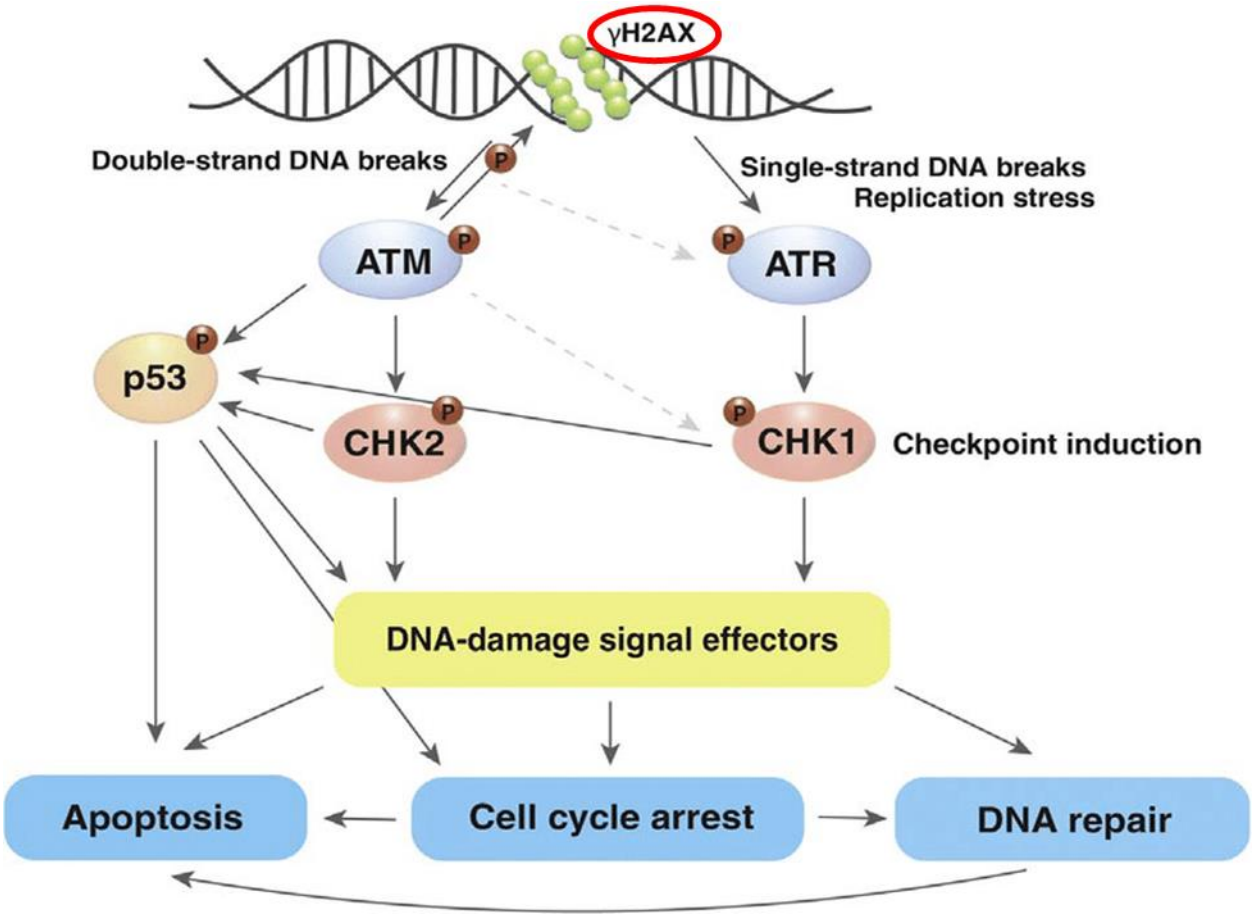

Figure 4- 1. The DNA damage response mechanism, shown in simplified form. DNA double-strand and single-strand breaks caused by DNA damage and replication stress activate ATM and ATR kinases, respectively. ATM and ATR are important downstream DDR signal transducers. They activate downstream cell-cycle regulators CHK1 and CHK2, which signal downstream checkpoints that halt the cell-cycle progression and activate DNA damage repair and tolerance mechanisms once phosphorylated. ATM also phosphorylates H2AX, which increases the signal of DNA damage. Furthermore, DDR activates the tumor suppressor p53, an essential DNA damage sensor that regulates cell fate based on DNA damage levels or DNA repair effectiveness. (Tšuiko et al., 2019).

The HCS DNA Damage Kit was created to simultaneously quantify two cell health indices, DNA damage ability, and cytotoxicity, in the same cell using high content screening. There are three indicators included in HCS DNA Damage Kit: an antibody against

phosphorylated H2AX, Hoechst33342, and Image-iT® DEAD Green™ viability marker. Precise antibody-based identification of phosphorylated H2AX (Ser139) in the nucleus is used to assess DNA damage as a sign of DNA double stand break. As a differentiation tool for automatic image processing, the package includes Hoechst33342, which stains nuclear DNA in living and dead cells. The Image-iT® DEAD Green™ viability marker has been used to assess cytotoxicity. The Image-iT® DEAD Green™ viability stain binds to DNA with a high affinity, is non-fluorescent, and impermeant, but when attached to DNA, produces highly fluorescent and stable dye-nucleic acid complexes. The impermeability of the plasma membrane to the dye prevents nuclear DNA staining in living cells. Drugs and test chemicals that cause severe cell damage, such as permeability of the plasma membrane, enable the Image-iT® DEAD Green™ viability stain to enter. With Image-iT® DEAD Green™ viability stain, this feature detects dead cells (Feng et al., 2018). In summary, the HCS DNA Damage Kit detects phosphorylated H2AX with a secondary antibody conjugate, detects cytotoxicity with Image-iT® DEAD Green™ dye, and labels nuclei in both living and dead cells with Hoechst^{TM} 33342 dye.

4.2 Materials and Experimental Protocol of the HCS DNA Damage assay

Two human pancreatic cancer cell lines (BxPC-3; PANC-1) and the normal human skin diploid fibroblast cell line (GM05757) were investigated to test DNA double-strand break and cell membrane permeability by the HCS DNA Damage assay. For the preparation of the HCS DNA Damage assay, all cell lines are stored and harvested under the same conditions as mentioned in Chapter 2 for the MTT assay.

There are four kinds of components included in the HCS DNA Damage Kit (Invitrogen, storage under -20 ˚C): Image-iT Dead Green™ viability stain as component A, pH2AX mouse monoclonal antibody as component B, Alexa Fluor® 555 goat anti-mouse IgG (H+L) as component C and Hoechst 33342 as component D. Three different characteristics of in vitro cell samples are stained to be visualized through respective filters. Before performing the assay, adherent cells were plated in optimize density and appropriate cell culture medium one day before adding the designed compounds. After 48 hrs treatment, six agents of HCS DNA damage detection are prepared as the following solution and appropriate concentration: dilution component A in complete cell culture medium (0.3 μM); fixative solution of 4% paraformaldehyde in phosphate-buffered saline; permeabilization solution of 0.25% Triton® X-100 in phosphate-buffered saline; blocking buffer of bovine serum albumin in PBS (10 mg/mL); dilution of component B diluted in blocking buffer (1 μg/mL); dilution of component C and D in blocking buffer (1 μg/mL and 1.67 μg/mL).

After solutions are ready for use, incubation medium keeps in all wells of 96-well plate while 50 μL of Image-iT® Dead Green™ viability stain working solution, bringing the total

volume to 150 µL and incubate the plate for 30 minutes under normal cell culture conditions. After that, all the medium is removed, and 100 mL of fixative solution is added to each well. After 15 mins incubation at RT, the solution is removed, and rinses wells once with PBS. The 100 µL permeabilization solution will be added in wells and incubate with the sample for 15 minutes at room temperature, then the cell samples are removed and washed with PBS. In each well of the plate, 100 µL blocking buffer incubate at room temperature. After 60 minutes and empty plates, 50 microlitres of primary antibody solution (H2AX) are added, and the plates are incubated at RT for 60 minutes. Rinsing wells three times with PBS, the prepared the secondary antibody/counterstain (Alexa Fluor®, Hoechst 33342) solution (50 µL/well), protecting from light for 60 minutes at room temperature. Wells are washed three times with PBS in the last step, and 100 mL of PBS is kept in each well for imaging and analysis. The nucleus is characterized by Hoechst 33342 in the Hoechst channel. The nucleus fluorescence intensity of Image-iT® DEAD Green™ viability stain with FITC/XF93 filters is used to determine cell membrane permeability. The signal fluorescence intensity of the pH2AX is evaluated using TRITC/ XF93 filters to assess DNA damage. Since the cell sample in each well is washed four times by phosphate-buffered saline during the process, cells need to be treated under appropriate conditions that can cause enough DNA DSB in the cell and maintain the cells' ability to adhere to the bottom wall of wells. Several preparation sets were designed to obtain the optimized cell number/well, drug concentration gradient, and treatment period.

4.3 Induced DNA DSB and Cytotoxicity Test of FMD Treatment by HCS DNA Damage Assay

For both human pancreatic cancer cell line BxPC-3 and PANC-1, 8000 cells were seeded into each well on black 96-well plates for overnight incubation. For optimal performances, cells were treated with various concentrations from 0 μM to 120 μM of FMD compound with the vehicle for 48 hours before the Double-Strand Breaks measurement was performed. This study determined if the FMD compound induces DNA damage in vitro using phosphorylated pH2AX (γH2AX) and Hoechst 33342 labeling. A combination of images obtained at Ex/Em of BP510-560/LP590 nm for Alexa Fluor® (double-strand break labeling) and those taken at BP330-380/LP420 nm for Hoechst 33342 (nucleic labeling) were used to create this composite image. Figure 4-2 shows images of double-strand break (red) and cell nuclei (blue), and the combined images of the exact location from different groups.

As shown in Figure 4-2 for the result of BxPC-3, there are significantly induced DNA DSB, which clearly can be seen from 30 μM of FMD compound. The majority of BxPC-3 cells have induced DNA damage after being treated by 120 μM FMD compound, which has a high potential for apoptosis eventually. From 0 μM control group to 120 μM high dose of FMD agent, the induced DNA double-strand breaks inside the nucleus is positively related with the drug concentration.

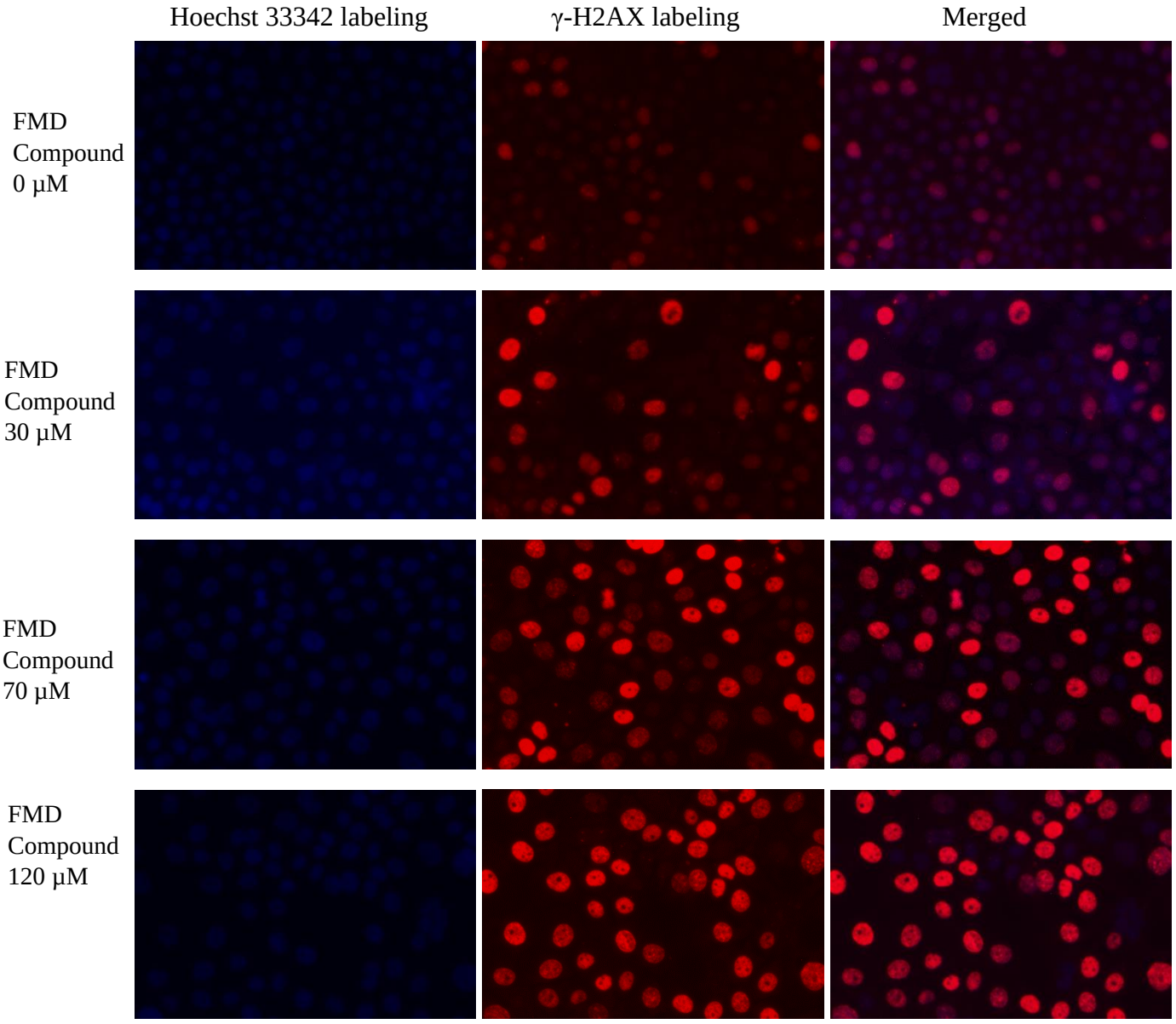

Figure 4- 2 Anti-Cancer Effect test: BxPC-3 Test by DNA DSB measurement treated by FMD compound for 48 hours, BxPC-3 cells were double-stained with Alexa Fluor® 555 (red, characterize DNA Double-strand break, exposure 30s) and Hoechst 33342 (blue, characterize cell nucleus, exposure 30s)

The images of DNA DSB were quantitatively analyzed by ImageJ software to compare between the experimental group (FMD agent) and the control group (vehicle).

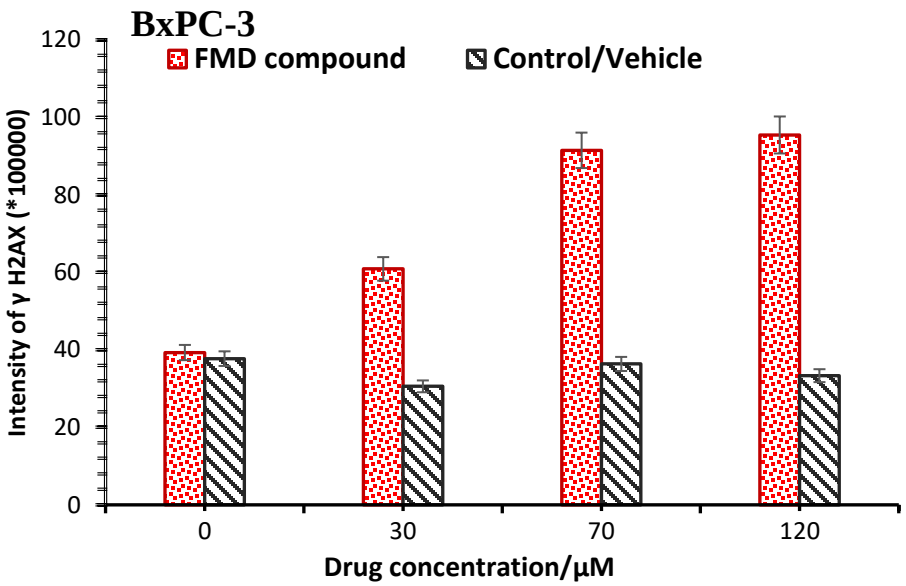

Figure 4- 3 The fluorescence intensity of γ-H2AX (Alexa Fluor® 555) versus FMD agent concentration of 0 μM, 30 μM, 70 μM, and 120 μM in BxPC-3 cells using the HCS DNA damage kit (by ImageJ)

The Intensity of γ-H2AX (Alexa Fluor) is measured by the ImageJ program. The intensity of images is represented by the integrated density of gray value, which indicates the brightness of a pixel. The quantitative analysis result illustrates that the FMD compound dramatically induced increasing DNA double-strand break to cancer cell line (BXPC-3) with increasing drug concentration. In contrast, the vehicle group did not cause any increasing DNA double stand break.

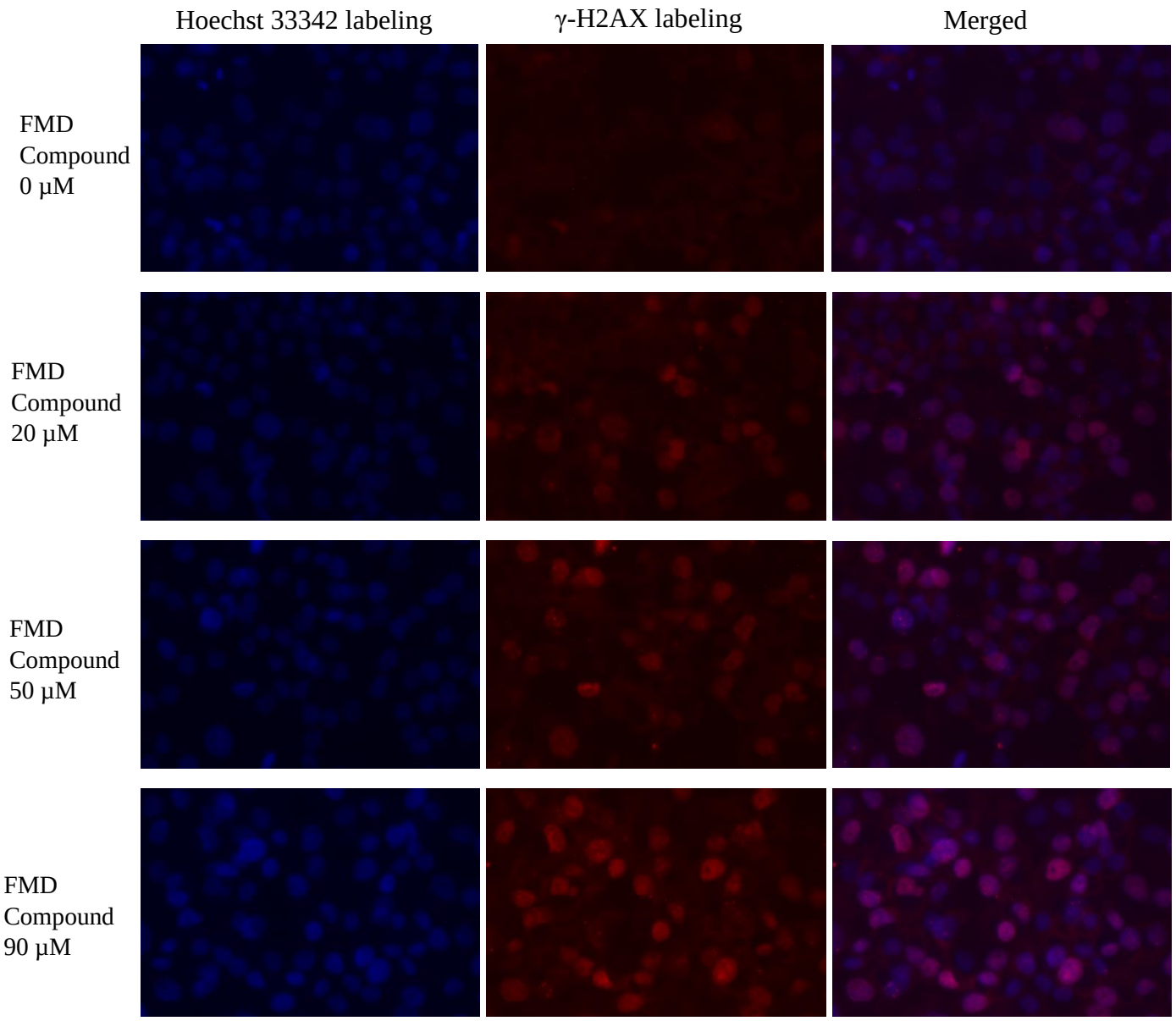

Figure 4- 4 Anti-Cancer Effect test: PANC-1 Test by DNA DSB measurement treated by FMD compound for 48 hours. PANC-1 cells were double-stained with Alexa Fluor® 555 (red, characterize DNA double-strand break, exposure 20s) and Hoechst 33342 (blue, represent cell nucleus, exposure 40s)

In the case of PANC-1, as shown in Figure 4-4, there are induced DNA double-strand breaks seen in the image at 20 µM of FMD compound, and the DNA damage indicator becoming more substantial when cells are treated with 90 µM FMD compound. A positive relationship

exists between the amount of DNA double-strand breaks produced within the nucleus and the concentration of FMD agent used, which ranges from 0 µM to 90 µM.

The images of DNA DSB were quantitatively examined using ImageJ software to compare the experimental group (containing the FMD agent) with the control group (including the vehicle).

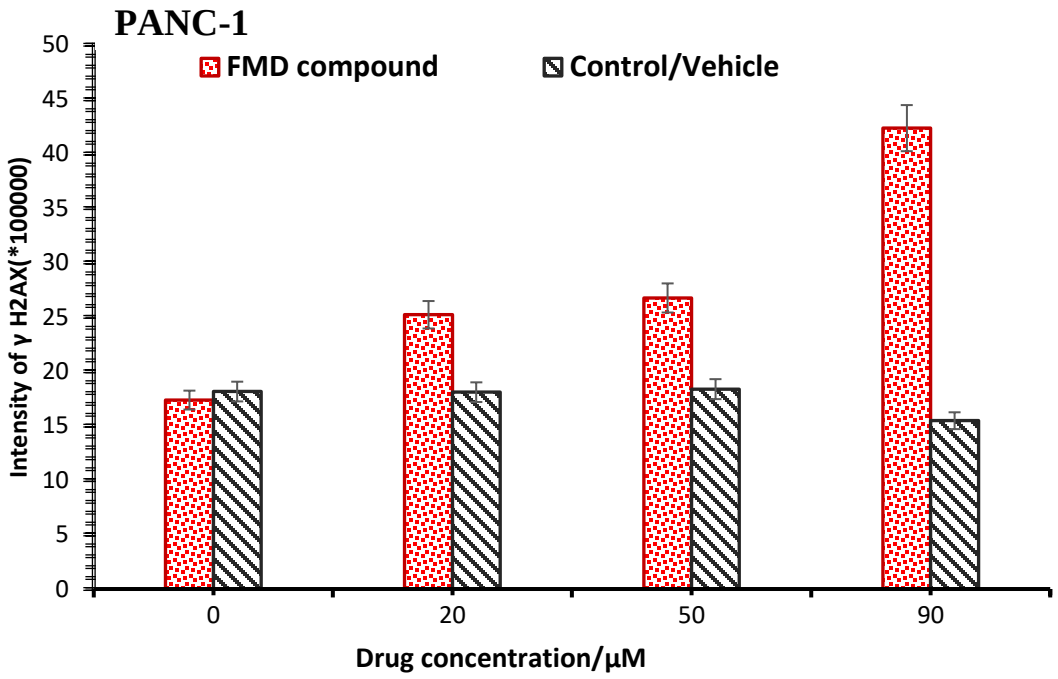

Figure 4- 5 The fluorescence intensity of γ-H2AX (Alexa Fluor® 555) versus FMD agent concentration of 0 µM, 30 µM, 70 µM and 120 µM in PANC-1 cells using the HCS DNA damage kit (measured by ImageJ)

The intensity of γ -H2AX (Alexa Fluor® 555) from the nucleus of PANC-1 cells is shown by the integrated density of grey value, representing the brightness of a pixel, in the same way as the quantitative result of BxPC-3 cell line is depicted.

From Figure 4-5, compared to the uninfluenced fluorescence intensity of the vehicle group, there is more DNA double-strand break induced by the FMD compound group to the human pancreatic cancer cell line (PANC-1) with increasing drug concentration.

Furthermore, the cytotoxicity of the FMD compound to the cancer cells and the normal human cell was also determined using the same kit, utilizing fluorescence image scanning acquired at BP450-490/LP520 nm for Image-iT® Dead Green™ staining. Only dead cells enable the Image-iT® Dead Green™ reagent to freely enter cells via a damaged cell membrane, which stains the DNA inside the cells. There were four concentrations of FMD chemicals in the gradient: 0, 30, 70, and 120 μM. Figure 4-6 depicts the GM05757 cell line, PANC-1 cell line, and BxPC-3 cell line. Cells with more severe membrane damage are represented by green cells that are brighter in color. It can be observed that the FMD compound did not affect the integrity of the cell membranes of normal skin cells from healthy humans. PANC-1 and BxPC-3 cells were extremely powerfully stained by Image-iT® Dead Green™, while GM05757 cells were faintly stained, as shown by the brilliant green hue of these cells. Therefore, from the images of Figure 4-6, the FMD compound potentially can distinguish pancreatic cancer cells from human normal skin cells and damage the membrane integrity of cancer cells.

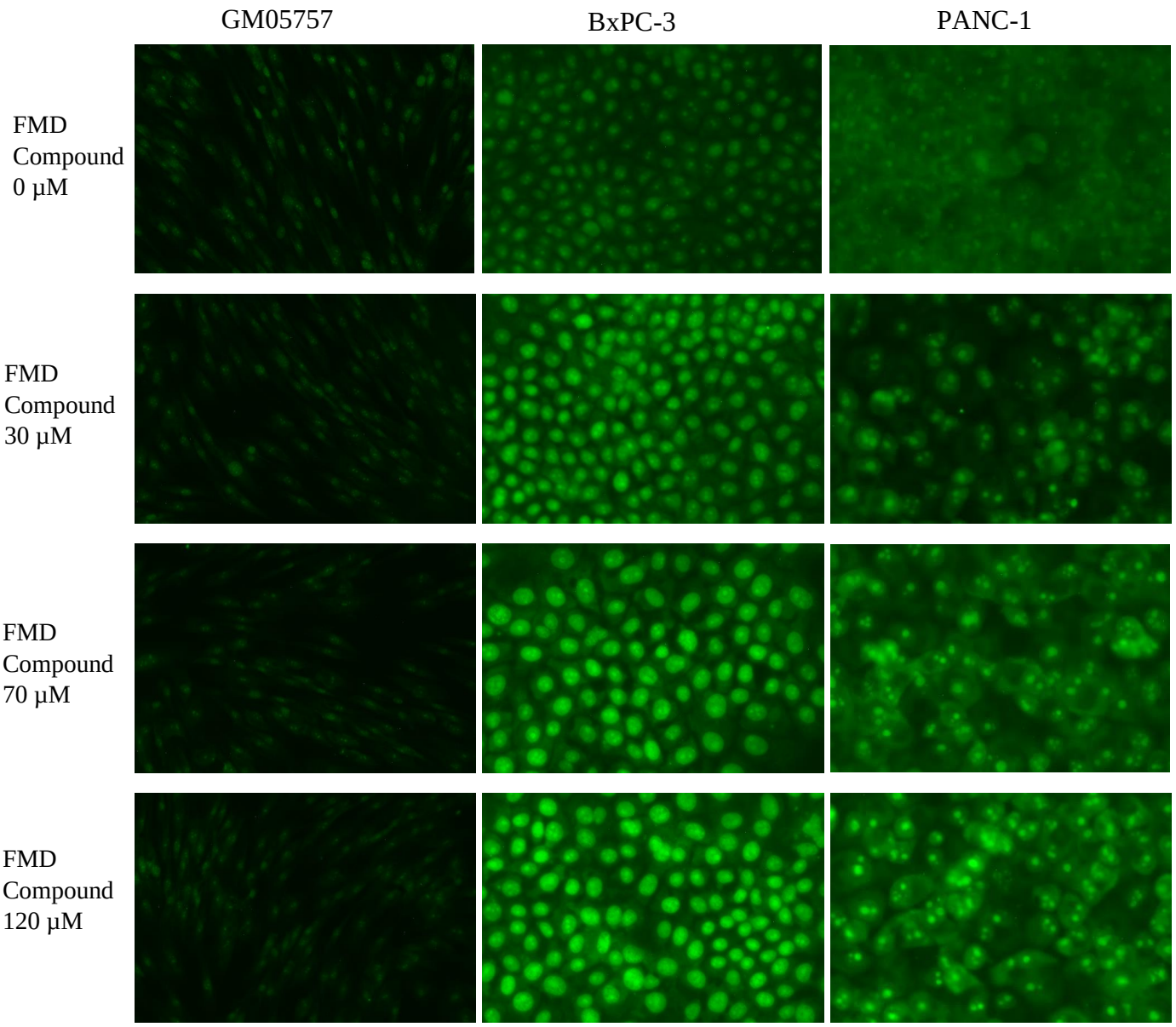

Figure 4- 6. Representative images of human normal skin and pancreatic cancer cells treated by FMD Compound for cytotoxicity evaluation using the HCS DNA damage kit. Cells were stained with Image-iT® Dead Green™

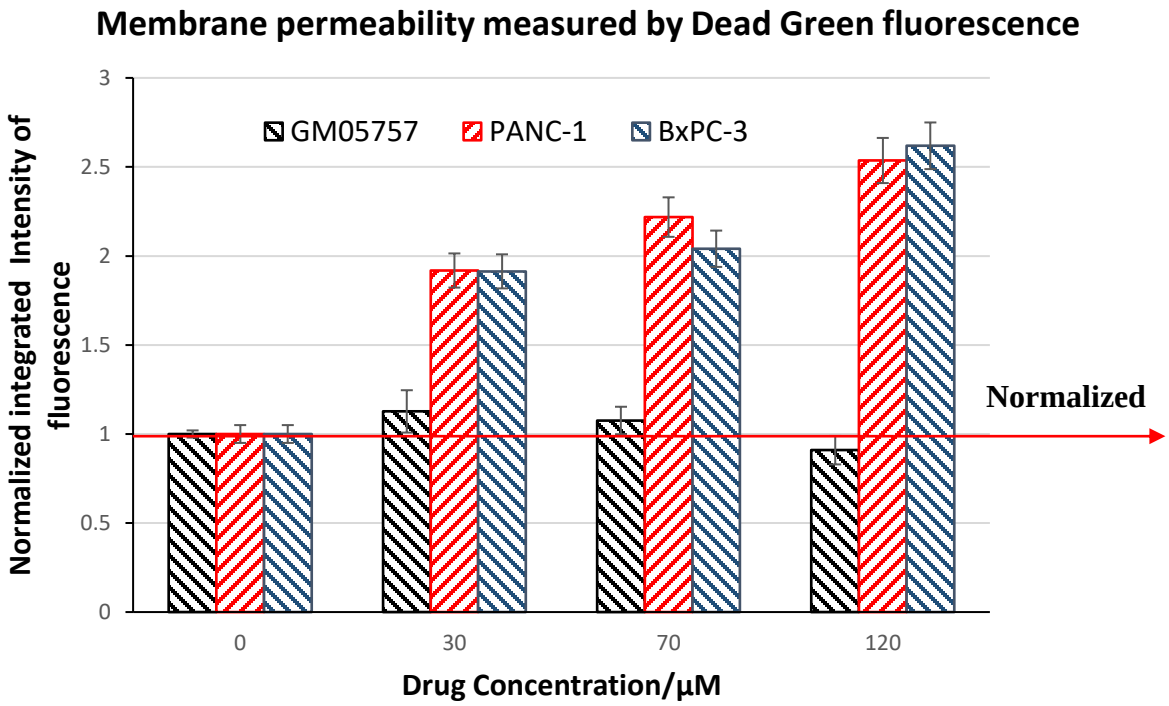

Figure 4- 7 Integrated Image-iT® Dead Green™ fluorescence intensity of GM05757/ PANC-1/BxPC-3 cells treated by FMD agent using the HCS DNA damage kit.

The Intensity of the Dead Green viability stain is measured by ImageJ software. For all three cell lines, the stained intensity is represented with the integrated density of gray value, which indicates the brightness of a pixel. Since the different morphology and characteristic of cell lines, the quantitative analysis of each cell line is normalized with the control group (0 µM FMD compound) of each experiment.

The quantitative analysis result of Image-iT® Dead Green™ fluorescence intensity demonstrates that the membrane permeability of pancreatic cancer cell lines (BxPC-3 & PANC-1) is positively related to the dose of FMD agent, which caused damage the cell membrane. On the other hand, for human normal cell line GM05757, the cell membrane maintains the same level of capacity to forbid the Image-iT® Dead Green™ staining going through and dye DNA. It

has been quantitatively illustrated that the FMD agent did not cause any severe damage to the GM05757 cell or influence its membrane permeability.

4.4 Conclusion from the DNA Damage Assay Results

In this Chapter, the anti-tumor effect of the FMD compound is evaluated from DNA damage measurement after the treatments to various cells.

The HCS DNA damage assay was used to measure the induced DNA damage and cytotoxicity of FMD compound from the DNA double-strand break and cell membrane permeability in cells after treatment which were indicated by fluorescent intensity. According to the results, γ-H2AX labeling images demonstrate the amount of DNA DSBs is intensified in pancreatic cancer cells with increasing concentrations of FMD compound. The intensity of the DNA DSB indicators increased by a factor of 2.5 with 120 μM (BxPC cell line) and 90 μM (PANC cell line) of the FMD compound. Dead Green viability-stained images show the FMD compound’s selective ability to damage the pancreatic cancer cell membrane instead of normal cells. When exposed to 120 μM of the FMD compound, pancreatic cancer cells' membrane permeability increased by more than 2.5 times compared with the control group, while human normal cell's membrane permeability stayed the same as the control group. Thus, the FMD compound has selective DNA damage ability and cytotoxicity to pancreatic cancer cells without severer damage to normal cells, which can be concluded that the FMD compound has a promising therapeutic effect on pancreatic cancer patients.

Chapter 5 Apoptosis measurements of pancreatic cancer cells after FMD Treatment through Caspase-3/7 Green Detection

Apoptosis cell staining, linked to caspase enzyme activity, may offer significant benefits for diagnosis, medication discovery, and treatment monitoring in various illnesses (Shim et al., 2017). Activated caspases and apoptotic cells were examined using a fluorescent microscope and the CellEvent™ Caspase-3/7 Green Detection Kit (Invitrogen). In this chapter, CellEvent™ Caspase-3/7 Green Detection will be introduced and applied to determine the apoptosis of designed compounds from Caspase-3/7 activation level in cells after treatment. The results of apoptosis measurement effectively illustrated the therapeutic efficacy and toxicity of Femto-medicine compound to PANC-1/ BxPC-3/ GM05757 cell lines (pancreatic cancer cell lines and human skin normal cell line).

5.1 Principles of Apoptosis measurements from Caspase-3/7 Green Detection

The programmed death of cells is known as apoptosis, which plays a critical role in many physiological functions; these include tissue homeostasis, embryonic development, immune system development, maintenance, and the disposal of damaged cells. (Sarvothaman et al., 2015) Morphologically, apoptosis is caused by chromatin condensation, nuclear fragmentation, and the loss of the mitochondrial inner transmembrane potential, which results in plasma membrane blebbing, with cells breaking into small membrane-surrounded fragments (apoptotic bodies) that are cleared by phagocytosis (Green & Reed, 1998). Many toxicants and chemotherapeutic drugs exert their mechanisms of action through the modulation of the

apoptosis process. Thus, interest in the apoptosis process and methods has grown steadily among toxicologists and other scientists (Lopez & Tait, 2015).

Caspase 3/7 activation is a hallmark of apoptosis in most cell systems, while the extrinsic and intrinsic apoptosis pathways lead to cell death via caspase-3 and caspase-7 cleavage. Caspase 3 controls DNA fragmentation and morphologic changes of apoptosis, whereas caspase 7 plays a minor role in these processes. In contrast, caspase 7 appears to be more important to the loss of cellular viability, although the combined role of both caspases is crucial in this area (Saquib et al., 2006). Consequently, quantification of apoptosis based on the extent of caspase 3/7 activation is preferred by most investigators (Bucur et al., 2012). Caspase 3/7 activity assays are the most frequently used apoptosis assays. Caspase 3/7 activity assays can be directly quantitated utilizing fluorescence or bioluminescence substrates in microplate reader formats.

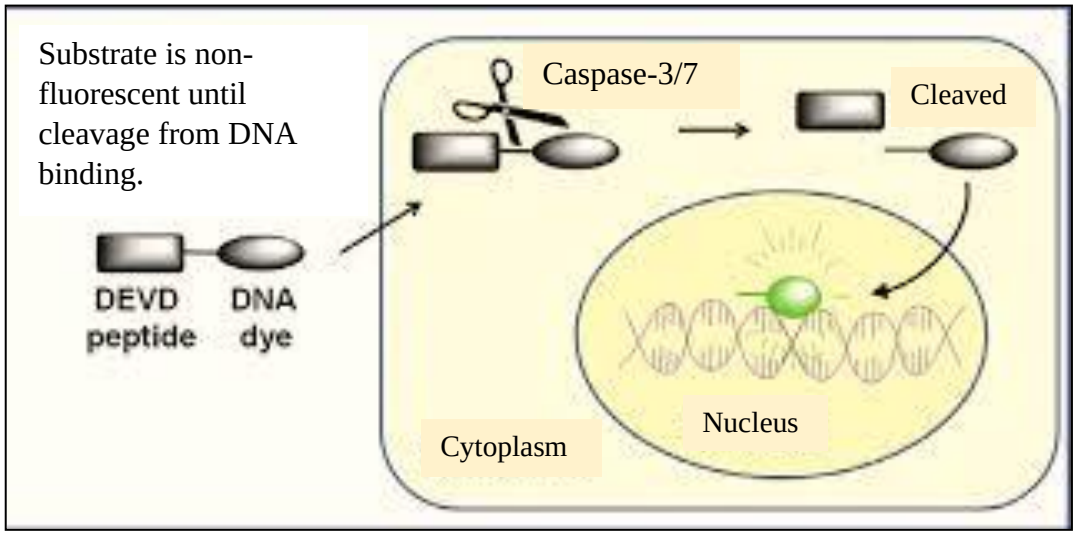

Figure 5- 1 Schematic showing the principle of the CellEvent™ Caspase-3/7 Green Detection Kit (Invitrogen)

CellEvent™ Caspase-3/7 Green Detection Reagent is an advanced fluorogenic substrate for the activated caspases 3/7 in apoptotic cells. In this reagent, a four-amino-acid peptide

(DEVD) is connected to a nucleic acid binding dye (Goode et al., 2010). Because the DEVD peptide prevents the dye from binding to DNA, this cell-permeable substrate is originally non-fluorescent. As shown in Figure 5-1, the DEVD peptide is cleaved after caspase-3 or caspase-7 activation in apoptotic cells, allowing the dye to attach to DNA and generate a solid fluorogenic reaction with an absorption/emission maximum of 502/530 nm.

To use this apoptosis detection reagent, add the substrate to cells sample in buffer or complete growth medium, incubate for 30 minutes, and validated for high-content imaging and analysis image. Apoptotic cells with activated caspase 3/7 show bright green nuclei, while cells without activated caspase 3/7 exhibit minimal fluorescence signal. Because the cleaved reagent labels nuclei, this stain can also provide information on nuclear morphology, including condensed nuclei typical of late-stage apoptosis (Goode et al., 2010). This assay has the advantage of not including wash stages, which helps retain the fragile apoptotic cells usually destroyed during wash steps (Bucur et al., 2012). It allows researchers to use high-dose therapy to trigger apoptotic cells with activated caspase 3/7 effectively.

5.2 Optimal Method of Caspase-3/7 Green Detection for experimental model

As an endpoint assay, CellEvent™ Caspase-3/7 Green Detection Reagent is applied to samples after cells are treated with the appropriate apoptotic inducer for the desired time (72 hrs). The detection reagent (2mM) is diluted into PBS with 5% FBS (Cat. Nos. 14040133 and 10082147) to a final concentration of 2 μM. Remove the media from wells, then add 100 μL of the diluted reagent to the cells in a 96-well plate. Put the plate in the incubator at 37°C for 30 minutes. Imaging the cells samples using the appropriate instrument filter for (502/530 nm) sets on the same day.

5.3 Apoptotic detection of FMD treated cell by Caspase-3/7 Green Detection Reagent

Apoptosis was detected in BxPC-3 cells using the CellEvent® Caspase-3/7 Green Detection Reagent (CellEvent®). Approximately 5000 cells/well were plated onto a black 96-well plate and left to incubate for one night. In order to optimize the apoptosis detection, the FMD agent is prepared to the concentration up to 500 μM to induce cell apoptosis efficiently, and without the wash step, the apoptotic cells will remain at the bottom of each well. The treatments with FMD compound were administered with concentrations gradient of 0, 100, 200, 300, 400, and 500 μM, and an incubation period of 72 hours. The control group was repeated simultaneously with the same procedures as the experimental group except the only the same volume of vehicles were added to the group (whose result was demonstrated in the quantitative result). Incubation with CellEvent® Caspase-3/7 Green Detection Reagent for 30 minutes resulted in the following images:

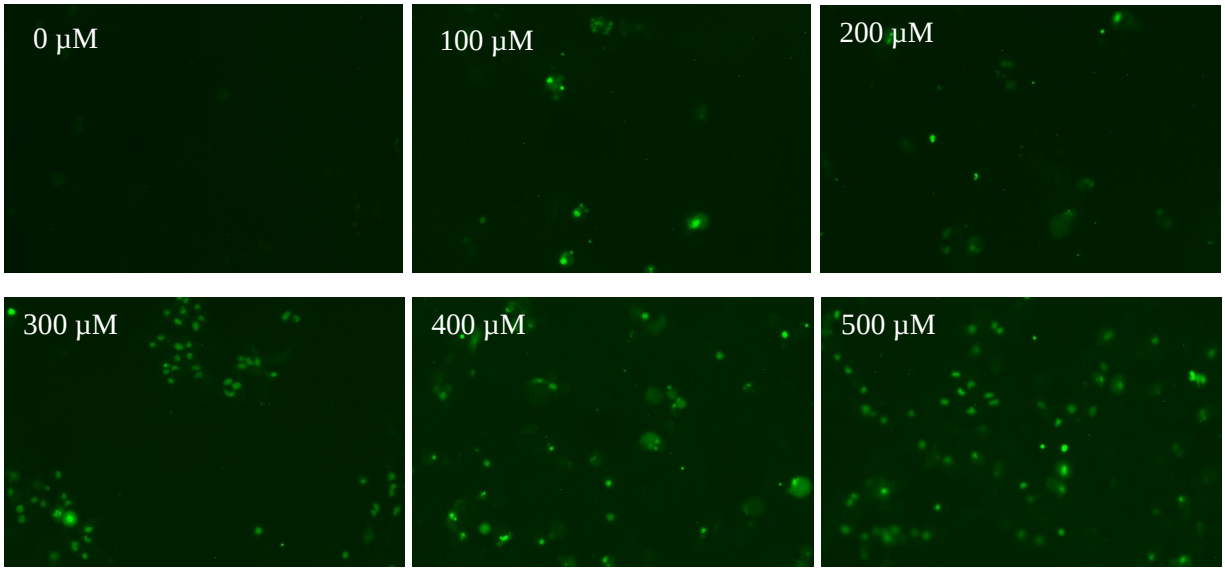

Figure 5- 2 Representative images of BxPC-3 cells treated by FMD Compound labeled by CellEvent® Caspase-3/7 Green Detection Reagent.

As illustrated in Figure 5-2, green cells indicate apoptotic BxPC-3 cells that have been activated, as shown by the Caspase 3/7 agent. By comparing the picture of the 0 mM FMD treated sample, it can be observed that more apoptotic cells (bright green particles) are present in higher dose groups.

The quantitative analyses were carried out by counting the number of green (apoptotic) cells using analyze particles function of ImageJ, and the results were represented by the number of apoptotic cells in each image with the same cell number seeded in each well before treatment was applied. As shown in Figure 5-3, the induced apoptotic BxPC-3 cell fast increased quantitatively with the higher concentration of the FMD compound. Compared to the control group, the number of apoptotic cells increased by around ten times at the FMD concentration of 500 µM. Compared with the treatment in the control group (vehicle), the treatment hardly induced more cells to apoptosis.

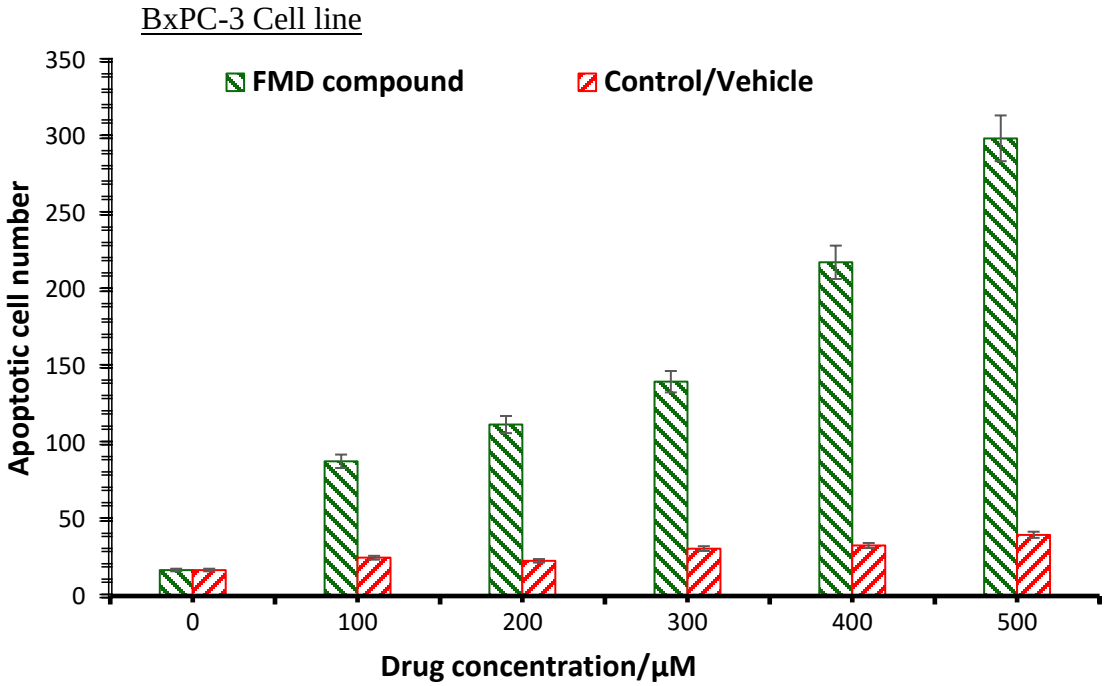

Figure 5- 3 The number of caspases 3/7 activated BxPC-3 pancreatic cancer cells with the same cell number seeded in each well before treatment (72hrs) applied. BxPC-3 pancreatic cancer cells were labeled by CellEvent® Caspase-3/7 Green Detection Reagent

The Apoptotic test was performed on the other pancreatic cancer cell line, PANC-1, using the same cell seeding number, drug concentration gradient, and the same vehicle group as the previous cell line. Figure 5-4 shows a fluorescence scanning image of apoptotic cells in the presence of a fluorescent dye. Besides, the images are quantitatively analyzed by ImageJ, then that result of PANC-1 is provided in Figure 5-5.

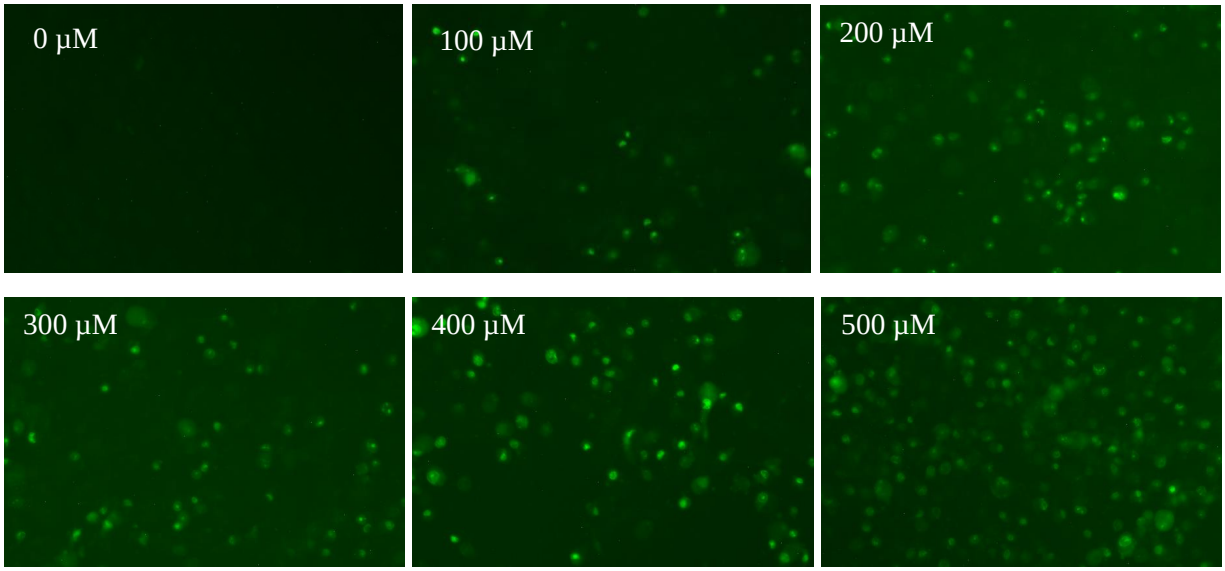

Figure 5- 4 Representative images of PANC-1 cells treated by FMD Compound labeled by CellEvent® Caspase-3/7 Green Detection Reagent.

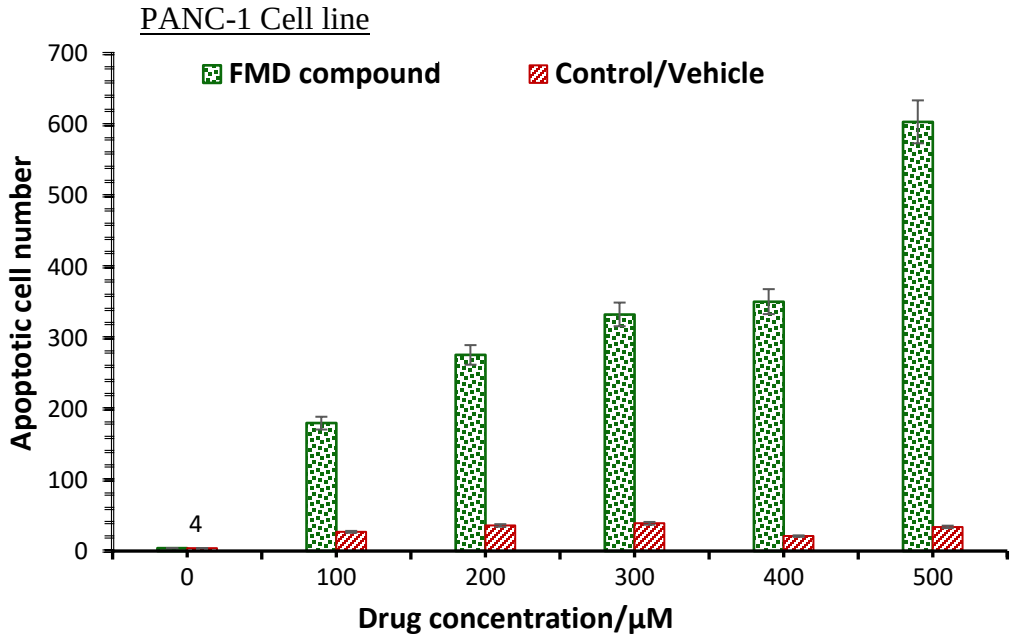

Figure 5- 5 The number of caspase-3/7 activated PANC-1 pancreatic cancer cells with the same cell number seeded in each well before treatment concentration. PANC-1 pancreatic cancer cells were labeled by CellEvent® Caspase-3/7 Green Detection Reagent

With similar results as the BxPC-3 cell line, there is an increasing number of green-dyed cells in images of FMD treated samples (Figure 5-4). The FMD agent induced significant apoptosis in PANC-1 cells with higher dosage. The quantitative result is also consistent. The apoptotic cell number increased around 15 times with 500 μM of FMD compound than the control group. Thus, the number of apoptotic cells increased dramatically with rising FMD compound dose, while the cell samples suffered mild harm from the vehicle.

5.4 Conclusion from the Apoptosis Measurement Results

This Chapter is aimed to determine the anti-tumor effect of the FMD compound from the induced apoptotic cell measurement after the treatments to various cells.

CellEvent™ Caspase-3/7 Green Detection was utilized to determine the induced apoptosis by FMD compound from Caspase-3/7 activation level in PANC-1/ BxPC-3/ GM05757 cell lines (pancreatic cancer cell lines and human skin normal cell line) after treatment. The Caspase-3/7 labeling fluorescent images and quantitative results illustrated that the pancreatic cancer cell lines are more apoptotic-sensitive to FMD compounds than human normal cells. It is verified that the anti-tumor effect of FMD compound to pancreatic cancer patients with the minor side effect.

Chapter 6 Conclusions and Further Discussion

In the current century, cancer is still significantly threatening human life quality and life expectance. Scientists have been researching cancer diagnosis and various therapies from the last century, and humans have implemented varieties of diagnostic instruments and medicines to treat cancer and extend the life of cancer patients. Pancreatic cancer stands out from the various types of cancer by the extremely high mortality (91%) within five years after diagnosis, which is one of the most aggressive human cancer. Most pancreatic cancer patients have limited appropriate treatment after being diagnosed at the late stage since there are no recognizable symptoms and signs in the early stage. Pancreatic cancer's survival rate is lagging in this rapidly cancer therapeutic research area. With scientific and clinical development, this disease remains aggressive and fatal, with a poor prognosis. Novel diagnostic and therapeutic methods are urgently needed for pancreatic cancer.

A discovery of femtomedicine by Dr. Qing-bin Lu and his group developed from the study of the mechanism of clinical cancer drugs. The DET (dissociative electron transfer reaction) reaction is recognized as the effective mechanism to react with weakly bound electrons (richly existing in the cancer cells) to produce reactive halogen species (RHS) and reactive radicals, which can lead to DNA damage in the cancer cells (Lu et al., 2015). FMD agents, a family of non-platinum-based anti-tumor agents, are capable of initiating the DET reaction with e_{pre}^- in cancerous cells and then induce the DNA DSB and death of cancer cells. There is in vitro and in vivo experimental evidence that FMD compounds at non-toxic have high therapeutic effects on different kinds of cancers, such as breast cancer, ovarian cancer, and lung cancer (Lu et al., 2015; Wang et al., 2016).

Furthermore, as an aggressive cancer type with the lowest survival rate, pancreatic cancer is increasingly getting noticed for developing more effective therapy. A study in Germany (Goetze et al., 2019) has confirmed that an FMD compound decreased the cell viability of some murine and human pancreatic cancer cells. Drug resistance is a significant barrier in clinical oncology and a problem to pancreatic cancer's current treatment. In this study of pancreatic cancer, more representative in vitro cell-based methods were applied to evaluate the anti-tumor efficiency to pancreatic cancer and the toxicity of one of the FMD compounds (1,2-Diamino-4,5-dibromobenzene, FMD-2Br-DAB). Different treatment conditions to cell lines are designed for different in vitro assays according to the characteristic of each assay, in order to optimize the cellular responses to the FMD compound from different aspects.

The results of the MTT assay indicated that the FMD compound increasingly killed pancreatic cancer cells with rising FMD doses, and the FMD compound successfully reduced the viability of pancreatic cancer cells by over 50% at a concentration of 300 μM FMD. It also showed no drug resistance existing in FMD treated groups, while all three tested pancreatic cancer cell lines show resistance to high dosages of Gemcitabine. These provide a possible solution to drug resistance in clinical cancer treatment. Besides, the negligible effect on cell viability of the normal cell line with FMD compound treatment (remains 80% at 300 μM) confirmed the low toxicity of this drug. The clonogenic assay is applied to access the cellular proliferation capacity of pancreatic cancer cell lines and human normal cell lines after being treated by FMD agents. The FMD compound inhibited colony-forming ability over 60% of the pancreatic cancer cells and less than 20 % of the human normal cells at the concentration of 50 μM FMD. The higher concentration of the FMD compound progressively damages the reproductive ability of pancreatic cancer cell lines, and it has minor effects on the proliferation

of normal cells. The rest two measurements with fluorescence-staining were directly visualized indications about DNA double-strand break, cell membrane permeability, and cell apoptosis. Two fluorescence scanning images (stained all cell nucleus and DNA DSB) were merged and illustrated the proportion of induced irreparable DNA damage. Observing the images demonstrated that the presence of the FMD compound significantly increased DNA DSB in pancreatic cancer cells. The yield of the DNA DSB in pancreatic cancer cell lines increased by a factor of 2.5 with the FMD compound at 90-120 μM. From the results of detecting cell membrane damage, the intensity of membrane permeability indicator increased by more than 2.5 times in the pancreatic cancer cells with 120 μM of the FMD compound, and no change in human normal cells is observed. The FMD agent selectively damaged the pancreatic cancer cells instead of human normal cells. Moreover, in the apoptosis detection results, the larger dose of FMD compound induced more significant activation of caspase-3/7 in pancreatic cancer cells. The apoptotic cell number increased about 10 to 15 times at the FMD concentration of 500 μM compared with the control group, and the quantity of induced apoptotic cells showed a dose-dependent manner to the FMD compound.

Based on the cell-based measurement of viability, reproductive ability, DNA DSB damage, cell membrane permeability, and apoptosis, all the results proved the competent antitumor effect on pancreatic cancer of the FMD agent with no appearance of drug resistance or significant side effects. From the evaluation of four different characteristics of cells, it can be concluded that the FMD agent has a high potential to become a chemotherapeutic treatment for pancreatic cancer.

Future research is anticipated that the results of this study's in vitro assessment will be applicable to in vivo animal models of pancreatic cancer, for instance, anti-cancer effect and

toxicity measurement to xenograft mouse models established by pancreatic tumor cell inoculations. Moreover, the FMD compound is expected to proceed to future clinical trials for the treatment of cancer patients, bringing the breakthrough of cancer chemotherapy in clinical oncology.

Bibliography

1. Siegel, M. (2020). Cancer statistics, 2020. CA: a Cancer Journal for Clinicians, 70(1), 7–30. https://doi.org/10.3322/caac.21590
2. Bray, F., Ferlay, J., Soerjomataram, I., Siegel, R. L., Torre, L. A. & Jemal, A. (2018). Global cancer statistics 2018: GLOBOCAN estimates of incidence and mortality worldwide for 36 cancers in 185 countries. *CA: A Cancer Journal for Clinicians*, 68: 394-424. doi:10.3322/caac.21492
3. Brenner, W. (2020). Projected estimates of cancer in Canada in 2020. *Canadian Medical Association Journal (CMAJ)*, *192*(9), E199–E205. https://doi.org/10.1503/cmaj.191292
4. Hallquist Viale, R. (2020). The American Cancer Society's Facts & Figures: 2020 Edition. Journal of the Advanced Practitioner in Oncology, 11(2). https://doi.org/10.6004/jadpro.2020.11.2.1
5. Ferlay, J., Soerjomataram, I., Dikshit, R., Eser, S., Mathers, C., Rebelo, M., Parkin, D. M., Forman, D., & Bray, F. (2015). Cancer incidence and mortality worldwide: sources, methods and major patterns in GLOBOCAN 2012. *International journal of cancer*, *136*(5), E359–E386. https://doi.org/10.1002/ijc.29210
6. Hanahan, W. (2011). Hallmarks of Cancer: The Next Generation. *Cell (Cambridge)*, *144*(5), 646–674. https://doi.org/10.1016/j.cell.2011.02.013
7. de Wit, S., van Dalum, G., & Terstappen, L. W. M. M. (2014). Detection of Circulating Tumor Cells. *Scientifica (Cairo)*, *2014*(819362), 819362–11. https://doi.org/10.1155/2014/819362
8. Coghlin, M. (2010). Current and emerging concepts in tumour metastasis. *The Journal of Pathology*, *222*(1), 1–15. https://doi.org/10.1002/path.2727

9. Hawkes, N. (2019). Cancer survival data emphasise importance of early diagnosis. *BMJ (Clinical Research Ed.), 364*, l408–l408. https://doi.org/10.1136/bmj.l408
10. Chien, P. (2017). Ovarian Cancer Prevention, Screening, and Early Detection: Report From the 11th Biennial Ovarian Cancer Research Symposium. *International Journal of Gynecological Cancer*, *27*(9S Suppl 5), S20–S22. https://doi.org/10.1097/IGC.0000000000001118
11. Histed, L. (2012). Review of functional/anatomical imaging in oncology. Nuclear Medicine Communications, 33(4), 349–361. https://doi.org/10.1097/MNM.0b013e32834ec8a5
12. Sauer, S. (2019). Current Prevalence of Major Cancer Risk Factors and Screening Test Use in the United States: Disparities by Education and Race/Ethnicity. *Cancer Epidemiology, Biomarkers & Prevention*, *28*(4), 629–642. https://doi.org/10.1158/1055-9965.EPI-18-1169
13. AENKER, Z. (2013). Serologic Autoantibodies as Diagnostic Cancer Biomarkers—A Review. *Cancer Epidemiology, Biomarkers & Prevention*, *22*(12), 2161–2181. https://doi.org/10.1158/1055-9965.EPI-13-0621
14. Stephan, J. (2007). PSA and other tissue kallikreins for prostate cancer detection. *European Journal of Cancer (1990)*, *43*(13), 1918–1926. https://doi.org/10.1016/j.ejca.2007.06.006
15. Brooks, M. (n.d.). Breast Cancer Screening and Biomarkers. *Cancer Epidemiology*, 307–321. https://doi.org/10.1007/978-1-60327-492-0_13

16. Bracci, Z. (2012). Serum autoantibodies to pancreatic cancer antigens as biomarkers of pancreatic cancer in a San Francisco Bay Area case–control study. *Cancer*, *118*(21), 5384–5394. https://doi.org/10.1002/cncr.27538

17. Ritchie, H. & Roser, M. (2018). *Causes of Death.* OurWorldInData.org. https://ourworldindata.org/causes-of-death

18. Wolfgang, H. (2013). Recent progress in pancreatic cancer. *CA: a Cancer Journal for Clinicians*, *63*(5), 318–348. https://doi.org/10.3322/caac.21190

19. Zhang, S. (2018). Challenges in diagnosis of pancreatic cancer. *World Journal of Gastroenterology : WJG*, *24*(19), 2047–2060. https://doi.org/10.3748/wjg.v24.i19.2047

20. Felsenstein, M., Hruban, R. H., & Wood, L. D. (2018). New Developments in the Molecular Mechanisms of Pancreatic Tumorigenesis. *Advances in anatomic pathology*, *25*(2), 131–142. https://doi.org/10.1097/PAP.0000000000000172

21. Mizrahi, J. D., Surana, R., Valle, J. W., & Shroff, R. T. (2020). Pancreatic cancer. *The Lancet (British Edition)*, *395*(10242), 2008–2020. https://doi.org/10.1016/S0140-6736(20)30974-0

22. Blausen.com staff (2014). Medical gallery of Blausen Medical 2014. *WikiJournal of Medicine* **1** (2). DOI:10.15347/wjm/2014.010. ISSN 2002-4436.

23. Stratton, C. (2009). The cancer genome. *Nature (London)*, *458*(7239), 719–724. https://doi.org/10.1038/nature07943

24. Singhi, K. (2019). Early Detection of Pancreatic Cancer: Opportunities and Challenges. *Gastroenterology (New York, N.Y. 1943)*, *156*(7), 2024–2040. https://doi.org/10.1053/j.gastro.2019.01.259

25. Caldwell, D. (2012). Cellular features of senescence during the evolution of human and murine ductal pancreatic cancer. *Oncogene*, *31*(12), 1599–1608. https://doi.org/10.1038/onc.2011.350

26. Kanda, M. (2012). Presence of Somatic Mutations in Most Early-Stage Pancreatic Intraepithelial Neoplasia. *Gastroenterology (New York, N.Y. 1943)*, *142*(4), 730–733.e9. https://doi.org/10.1053/j.gastro.2011.12.042

27. Guo, X. (2016). Molecular Biomarkers of Pancreatic Intraepithelial Neoplasia and Their Implications in Early Diagnosis and Therapeutic Intervention of Pancreatic Cancer. *International Journal of Biological Sciences*, *12*(3), 292–301. https://doi.org/10.7150/ijbs.14995

28. Hosoda, C. (2017). Genetic analyses of isolated high-grade pancreatic intraepithelial neoplasia (HG-PanIN) reveal paucity of alterations in TP53 and SMAD4. *The Journal of Pathology*, *242*(1), 16–23. https://doi.org/10.1002/path.4884

29. Amato, M. (2014). Targeted next-generation sequencing of cancer genes dissects the molecular profiles of intraductal papillary neoplasms of the pancreas. *The Journal of Pathology*, *233*(3), 217–227. https://doi.org/10.1002/path.4344

30. Kanda, S. (2013). Mutant TP53 in Duodenal Samples of Pancreatic Juice from Patients With Pancreatic Cancer or High-Grade Dysplasia. *Clinical Gastroenterology and Hepatology*, *11*(6), 719–730.e5. https://doi.org/10.1016/j.cgh.2012.11.01

31. Feigin, G. (2017). Recurrent noncoding regulatory mutations in pancreatic ductal adenocarcinoma. *Nature Genetics*, *49*(6), 825–833. https://doi.org/10.1038/ng.3861

32. Garrido-Laguna, H. (2015). Pancreatic cancer: from state-of-the-art treatments to promising novel therapies. *Nature Reviews. Clinical Oncology*, *12*(6), 319–334. https://doi.org/10.1038/nrclinonc.2015.53

33. Saung, Z. (2017). Current Standards of Chemotherapy for Pancreatic Cancer. *Clinical Therapeutics*, *39*(11), 2125–2134. https://doi.org/10.1016/j.clinthera.2017.08.015

34. Roth, C. (2020). Recent advances in the treatment of pancreatic cancer [version 1; peer review: awaiting peer review]. *F1000Research*, *9*, 131–. https://doi.org/10.12688/f1000research.21981.1

35. Croome, F. (2014). Total Laparoscopic Pancreaticoduodenectomy for Pancreatic Ductal Adenocarcinoma: Oncologic Advantages Over Open Approaches? *Annals of Surgery*, *260*(4), 633–640. https://doi.org/10.1097/SLA.0000000000000937

36. Conroy, H. (2018). FOLFIRINOX or Gemcitabine as Adjuvant Therapy for Pancreatic Cancer. *The New England Journal of Medicine*, *379*(25), 2395–2406. https://doi.org/10.1056/NEJMoa1809775

37. Tempero, M. A., Reni, M., Riess, H., Pelzer, U., O'Reilly, E. M., Winter, J. M., Oh, D.-Y., Li, C.-P., Tortora, G., Chang, H.-M., Lopez, C. D., Tabernero, J., Van Cutsem, E., Philip, P. A., Goldstein, D., Berlin, J., Ferrara, S., Li, M., Lu, B. D., & Biankin, A. (2019). APACT: phase III, multicenter, international, open-label, randomized trial of adjuvant nab-paclitaxel plus gemcitabine (nab-P/G) vs gemcitabine (G) for surgically resected pancreatic adenocarcinoma. Journal of Clinical Oncology, 37(15_suppl), 4000–4000. https://doi.org/10.1200/JCO.2019.37.15_suppl.4000

38. Ma, O. (2019). Association of Timing of Adjuvant Therapy With Survival in Patients With Resected Stage I to II Pancreatic Cancer. *JAMA Network Open*, *2*(8), e199126–e199126. https://doi.org/10.1001/jamanetworkopen.2019.9126

39. Hammel, H. (2016). Effect of Chemoradiotherapy vs Chemotherapy on Survival in Patients With Locally Advanced Pancreatic Cancer Controlled After 4 Months of Gemcitabine With or Without Erlotinib: The LAP07 Randomized Clinical Trial. *JAMA : the Journal of the American Medical Association*, *315*(17), 1844–1853. https://doi.org/10.1001/jama.2016.4324

40. Marthey, M. (2015). FOLFIRINOX for Locally Advanced Pancreatic Adenocarcinoma: Results of an AGEO Multicenter Prospective Observational Cohort. *Annals of Surgical Oncology*, *22*(1), 295–301. https://doi.org/10.1245/s10434-014-3898-9

41. Conroy, D. (2011). FOLFIRINOX versus Gemcitabine for Metastatic Pancreatic Cancer. *The New England Journal of Medicine*, 364(19), 1817–1825. https://doi.org/10.1056/NEJMoa1011923

42. Wang-Gillam, L. (2016). Nanoliposomal irinotecan with fluorouracil and folinic acid in metastatic pancreatic cancer after previous gemcitabine-based therapy (NAPOLI-1): a global, randomised, open-label, phase 3 trial. *The Lancet (British Edition)*, *387*(10018), 545–557. https://doi.org/10.1016/S0140-6736(15)00986-1

43. Riss, T. L., Moravec, R. A., Niles, A. L., Duellman, S., Benink, H. A., Worzella, T. J., & Minor, L. (2013). Cell Viability Assays. In S. Markossian (Eds.) et. al., *Assay Guidance Manual*. Eli Lilly & Company and the National Center for Advancing Translational Sciences.

44. Stockert, J., Blázquez-Castro, A., Cañete, M., Horobin, R., & Villanueva, Á. (2012). MTT assay for cell viability: Intracellular localization of the formazan product is in lipid droplets. Acta Histochemica, 114(8), 785–796. https://doi.org/10.1016/j.acthis.2012.01.006

45. Zhang, J., Wang, L., Xing, Z., Liu, D., Sun, J., Li, X., & Zhang, Y. (2010). Status of bi- and multi-nuclear platinum anticancer drug development. *Anti-cancer agents in medicinal chemistry*, *10*(4), 272–282. https://doi.org/10.2174/187152010791162270

46. Florea, A. M., & Büsselberg, D. (2011). Cisplatin as an anti-tumor drug: cellular mechanisms of activity, drug resistance and induced side effects. *Cancers*, *3*(1), 1351–1371. https://doi.org/10.3390/cancers3011351

47. Chen, D., Milacic, V., Frezza, M., & Dou, Q. P. (2009). Metal complexes, their cellular targets and potential for cancer therapy. *Current pharmaceutical design*, *15*(7), 777–791. https://doi.org/10.2174/138161209787582183

48. Nepomuceno, J. C. (2011). Antioxidants in Cancer Treatment, Current Cancer Treatment - Novel Beyond Conventional Approaches, Öner Özdemir, IntechOpen, DOI: 10.5772/23131. https://www.intechopen.com/chapters/24599

49. Wang, D., & Lippard, S. J. (2005). Cellular processing of platinum anticancer drugs. *Nature Reviews. Drug Discovery*, *4*(4), 307–320. https://doi.org/10.1038/nrd1691

50. Zewail, A. H. (2000). Femtochemistry: Atomic-Scale Dynamics of the Chemical Bond. *The Journal of Physical Chemistry. A, Molecules, Spectroscopy, Kinetics, Environment, & General Theory*, *104*(24), 5660–5694. https://doi.org/10.1021/jp001460h

51. Stolow, A., Bragg, A., & Neumark, D. (2004). Femtosecond time-resolved photoelectron spectroscopy. Chemical Reviews, 104(4), 1719-1757

52. Lu, Q. (2007). Molecular reaction mechanisms of combination treatments of low-dose cisplatin with radiotherapy and photodynamic therapy. Journal of Medicinal Chemistry, 50(11), 2601-4.

53. Lu, Q., Kalantari, S., & Wang, C. (2007). Electron transfer reaction mechanism of cisplatin with DNA at the molecular level. Molecular Pharmaceutics, 4(4), 624-628.

54. Lu, Q. (2010). Effects and applications of ultrashort-lived prehydrated electrons in radiation biology and radiotherapy of cancer. Mutation Research-Reviews in Mutation Research, 704(1), 190-199.

55. Goetze, R. G., Buchholz, S. M., Ou, N., Zhang, Q., Patil, S., Schirmer, M., Singh, S. K., Ellenrieder, V., Hessmann, E., Lu, Q.-B., & Neesse, A. (2019). Preclinical Evaluation of 1,2-Diamino-4,5-Dibromobenzene in Genetically Engineered Mouse Models of Pancreatic Cancer. *Cells (Basel, Switzerland)*, *8*(6), 563–. https://doi.org/10.3390/cells8060563

56. Zhang, Q., & Lu, Q.-B. (2021). New combination chemotherapy of cisplatin with an electron-donating compound for treatment of multiple cancers. *Scientific Reports*, *11*(1), 788–13. https://doi.org/10.1038/s41598-020-80876-z

57. Luo, T., Yu, J., Nguyen, J., Wang, C.-R., Bristow, R. G., Jaffray, D. A., Zhou, X. Z., Lu, K. P., & Lu, Q.-B. (2012). Electron transfer-based combination therapy of cisplatin with tetramethyl-p-phenylenediamine for ovarian, cervical, and lung cancers. *Proceedings of the National Academy of Sciences - PNAS*, *109*(26), 10175–10180. https://doi.org/10.1073/pnas.1203451109

58. Mosmann, T. (1983). Rapid colorimetric assay for cellular growth and survival: Application to proliferation and cytotoxicity assays. *Journal of Immunological Methods*, *65*(1), 55–63. https://doi.org/10.1016/0022-1759(83)90303-4

59. Berridge, M. V., Herst, P. M., & Tan, A. S. (2005). Tetrazolium dyes as tools in cell biology: new insights into their cellular reduction. Biotechnology annual review, 11, 127–152. https://doi.org/10.1016/S1387-2656(05)11004-7

60. Hansen, M. B., Nielsen, S. E., & Berg, K. (1989). Re-examination and further development of a precise and rapid dye method for measuring cell growth/cell kill. *Journal of Immunological Methods*, *119*(2), 203–210. https://doi.org/10.1016/0022-1759(89)90397-9

61. Van Meerloo, J., Kaspers, G. J. L., & Cloos, J. (2011). Cell Sensitivity Assays: The MTT Assay. *Cancer Cell Culture*, 237–245. https://doi.org/10.1007/978-1-61779-080-5_20

62. Bahuguna, A., I. Khan, V. Bajpai, & S. Kang. (2017). MTT Assay to Evaluate the Cytotoxic Potential of a Drug. *Bangladesh Journal of Pharmacology, 12(2), p.* doi:10.3329/bjp.v12i2.30892.

63. Vincent, A., Herman, J., Schulick, R., Hruban, R. H., & Goggins, M. (2011). Pancreatic cancer. The Lancet (British Edition), 378(9791), 607–620. https://doi.org/10.1016/S0140-6736(10)62307-0

64. Deer, E. L., González-Hernández, J., Coursen, J. D., Shea, J. E., Ngatia, J., Scaife, C. L., Firpo, M. A., & Mulvihill, S. J. (2010). Phenotype and genotype of pancreatic cancer cell lines. *Pancreas*, *39*(4), 425–435. https://doi.org/10.1097/MPA.0b013e3181c15963

65. Tan, M. H., Nowak, N. J., Loor, R., Ochi, H., Sandberg, A. A., Lopez, C., Pickren, J. W., Berjian, R., Douglass, H. O., & Chu, T. M. (1986). Characterization of a New Primary

Human Pancreatic Tumor Line. *Cancer Investigation*, *4*(1), 15–23. https://doi.org/10.3109/07357908609039823

66. Lieber, M., Mazzetta, J., Nelson-Rees, W., Kaplan, M., & Todaro, G. (1975). Establishment of a continuous tumor-cell line (PANC-1) from a human carcinoma of the exocrine pancreas. *International Journal of Cancer*, *15*(5), 741–747. https://doi.org/10.1002/ijc.2910150505

67. Septisetyani, E., Ningrum, R., Romadhani, Y., Wisnuwardhani, P., & Santoso, A. (2014). Optimization of sodium dodecylsulphate as a formazan solvent and comparison of 3-(4,-5-dimethylthiazo-2-yl)-2,5-diphenyltetrazolium bromide (MTT) assay with WST-1 assay in MCF-7 cells. *Indonesian journal of pharmacy. 245(25)*. 10.14499/indonesianjpharm25iss4pp245.

68. Franken, N. A. P., Rodermond, H. M., Stap, J., Haveman, J., & van Bree, C. (2006). Clonogenic assay of cells in vitro. Nature Protocols, 1(5), 2315–2319. https://doi.org/10.1038/nprot.2006.339

69. Buch, K., Peters, T., Nawroth, T., Sänger, M., Schmidberger, H., & Langguth, P. (2012). Determination of cell survival after irradiation via clonogenic assay versus multiple MTT Assay--a comparative study. *Radiation Oncology (London, England)*, *7*(1), 1–1. https://doi.org/10.1186/1748-717X-7-1

70. Rafehi, H., Orlowski, C., Georgiadis, G. T., Ververis, K., El-Osta, A., & Karagiannis, T. C. (2011). Clonogenic assay: adherent cells. *Journal of visualized experiments : JoVE*, (49), 2573. https://doi.org/10.3791/2573

71. Nuryadi, E., Mayang Permata, T. B., Komatsu, S., Oike, T., & Nakano, T. (2018). Inter-assay precision of clonogenic assays for radiosensitivity in cancer cell line A549. *Oncotarget*, *9*(17), 13706–13712. https://doi.org/10.18632/oncotarget.24448

72. PUCK, T. T., & MARCUS, P. I. (1956). Action of x-rays on mammalian cells. *The Journal of Experimental Medicine*, *103*(5), 653–666. https://doi.org/10.1084/jem.103.5.653

73. Stoddart, M. J. (2011). *Mammalian cell viability methods and protocols* . Humana Pressr.

74. Munshi, A., Hobbs, M. & Meyn, Raymond. (2005). Clonogenic Cell Survival Assay. *Methods in molecular medicine. 110. 21-8*. 10.1385/1-59259-869-2:021.

75. Obeidat, M., McConnell, K. A., Li, X., Bui, B., Stathakis, S., Papanikolaou, N., Rasmussen, K., Ha, C. S., Lee, S. E., Shim, E. Y., & Kirby, N. (2018). DNA double‐strand breaks as a method of radiation measurements for therapeutic beams. Medical Physics (Lancaster), 45(7), 3460–3465. https://doi.org/10.1002/mp.12956

76. Garcia-Canton, C., Anadon, A., & Meredith, C. (2013). Assessment of the in vitro γH2AX assay by High Content Screening as a novel genotoxicity test. *Mutation Research. Genetic Toxicology and Environmental Mutagenesis*, *757*(2), 158–166. https://doi.org/10.1016/j.mrgentox.2013.08.002

77. Feng, J., Sa, Y., Huang, Z., & Feng, Y. (2018). Co-Localization Analysis Method for High Content Screening (HCS) Measurement of Radiation Induced DNA Damage Response. *International Journal of Radiation Oncology, Biology, Physics*, *102*(3), e156–e156. https://doi.org/10.1016/j.ijrobp.2018.07.606

78. Khanna, K. K., & Jackson, S. P. (2001). DNA double-strand breaks: signaling, repair and the cancer connection. *Nature Genetics*, *27*(3), 247–254. https://doi.org/10.1038/85798

79. Rich, T., Wyllie, A. H., & Allen, R. L. (2000). Defying death after DNA damage. *Nature (London)*, *407*(6805), 777–783. https://doi.org/10.1038/35037717

80. Tšuiko, O., Jatsenko, T., Parameswaran Grace, L. K., Kurg, A., Vermeesch, J. R., Lanner, F., Altmäe, S., & Salumets, A. (2019). A speculative outlook on embryonic aneuploidy: Can molecular pathways be involved? *Developmental Biology*, *447*(1), 3–13. https://doi.org/10.1016/j.ydbio.2018.01.014

81. Shim, M.K., Yoon, H.Y., Lee, S. Jo, M. K., Park, J., Kim, J., Jeong, S.Y., Kwon, I.C. & Kim, K. (2017). Caspase-3/-7-Specific Metabolic Precursor for Bioorthogonal Tracking of Tumor Apoptosis. *Scientific Reports* **7,** 16635 https://doi.org/10.1038/s41598-017-16653-2

82. Carrasco, R. A., Stamm, N. B., & Patel, B. K. . (2003). One-Step Cellular Caspase-3/7 Assay. *BioTechniques*, *34*(5), 1064–1067. https://doi.org/10.2144/03345dd02

83. Brentnall, M., Rodriguez-Menocal, L., De Guevara, R. L., Cepero, E., & Boise, L. H. (2013). Caspase-9, caspase-3 and caspase-7 have distinct roles during intrinsic apoptosis. *BMC Cell Biology*, *14*(1), 32–32. https://doi.org/10.1186/1471-2121-14-32

84. Porter, A. G., & Jänicke, R. U. (1999). Emerging roles of caspase-3 in apoptosis. *Cell Death and Differentiation*, *6*(2), 99–104. https://doi.org/10.1038/sj.cdd.4400476

85. Muganda, P. M. (2016). *Apoptosis Methods in Toxicology* (1st ed. 2016.). Springer New York. https://doi.org/10.1007/978-1-4939-3588-8

86. Sarvothaman, S., Undi, R. B., Pasupuleti, S. R., Gutti, U., & Gutti, R. K. (2015). Apoptosis: role in myeloid cell development. *Blood Research*, *50*(2), 73–79. https://doi.org/10.5045/br.2015.50.2.73

87. Lopez, J., & Tait, S. W. G. (2015). Mitochondrial apoptosis: killing cancer using the enemy within. *British Journal of Cancer*, *112*(6), 957–962. https://doi.org/10.1038/bjc.2015.85

88. Bucur, O., Stancu, A. L., Khosravi-Far, R., & Almasan, A. (2012). Analysis of apoptosis methods recently used in Cancer Research and Cell Death & Disease publications. *Cell Death & Disease*, *3*(2), e263–e263. https://doi.org/10.1038/cddis.2012.2

89. Green, D. R., & Reed, J. C. (1998). Mitochondria and Apoptosis. *Science (American Association for the Advancement of Science)*, *281*(5381), 1309–1312.